Detection of Bolt Stress Relaxation in Hybrid Bolted Connections

Project Report

by:

Richard Mewer, Graduate Research Assistant
Senthil S. Vel, Ph.D., Assistant Professor
and
Vincent Caccese, Ph.D. P.E., Associate Professor

Prepared for:

Office of Naval Research
800 N Quincy St.
Arlington VA. 22217-5660

Grant No. N00014-01-1-0916
Dr. Roshdy G.S. Barsoum,
Program Manager

University of Maine
Department of Mechanical Engineering
Orono, ME 04469-5711

Report No. UM-MACH-RPT-01-07

April 2003

TABLE OF CONTENTS

Page

ABSTRACT

The effort summarized in this report focuses upon real time detection of stress relaxation in bolted connections in hybrid structures. A proof-of-concept test bed for this effort consists of a 24-½ inch square plate made of Eglass/vinyl ester composite bolted to a steel framework. Several interrogation techniques were employed and compared including: 1) low frequency modal analysis; 2) high frequency transfer functions and 3) high frequency transmittance functions. Each of these techniques employed a piezoelectric actuator bonded to the panel to deliver a characterized disturbance in a controlled manner. Methods to detect bolt loosening were evaluated for effectiveness in detection of single bolt loosening, multiple bolt loosening and in determining the location of a loosened bolt. Techniques using high frequency input signals and transfer or transmittance functions were able to distinguish changes in a damage index. The technique using transmittance functions to evaluate changes in bolt tensioning level shows the most promise.

ACKNOWLEDGEMENTS

The authors gratefully acknowledge funding for this project through the Office of Naval Research under grant number N00014-01-1-0916. Dr. Roshdy G..S. Barsoum of ONR is the cognizant program officer. His support and encouragement is greatly appreciated. The authors would also like to thank Milt Crichfield, Loc Nguyen and Gene Camponeschi of NSWC Carderock (NSWCCD) for their assistance and advice. Furthermore, the support of the other partners involved in this effort, particularly, Steven Loui and Todd Pelzer of Pacific Marine, Navatek Division and Larry Thompson, Steve Webber and Ken Light of Applied Thermal Sciences. Assistance of support personnel in the Mechanical Engineering department is acknowledged, including Randy Bragg, Research Engineer, and Keith Berube who fabricated the test specimen and assisted in editing of this report.

1. INTRODUCTION

The research summarized in this report was performed under the Modular Advanced Composite Hull-form (MACH) project sponsored by the Office of Naval Research (ONR). The overall objective of the MACH program is to implement robust techniques leading toward the use of hybrid composite/metal construction in naval ship hull applications. The near term goal of MACH is to develop and demonstrate novel hybrid connection approaches and structural monitoring and evaluation methodologies for composite panels interfaced to metallic advanced hull-form structures.

The effort summarized in this report focuses upon real time detection of stress relaxation in bolted connections in hybrid structures. A proof-of-concept test bed for this effort consists of a 24-½ inch square plate made of Eglass/vinyl ester composite. The hybrid connection was formed by bolting this plate to a steel frame using sixteen ½ inch diameter steel bolts. Several interrogation techniques were employed and compared including: 1) low frequency modal analysis; 2) high frequency transfer functions and 3) high frequency transmittance functions. Each of these techniques employed a piezoelectric actuator bonded to the panel to deliver a characterized disturbance in a controlled manner. The technique using transmittance functions to evaluate changes in bolt tensioning level shows the most promise.

Robust methods used to ascertain bolt stress relaxation will be of much benefit in assessment of structural integrity in hybrid connections. Changes in bolt tension in a hybrid connection can be catastrophic if bolts loosen below a critical value. Bolt loosening in a ship structure may occur due to viscoelastic creep of the composite material, repetitive loading, overloading or environmental effects. A ship is a dynamically loaded vessel and mitigation of structural failures is essential. More often than not structural failures occur at connections and interfaces, and rarely occur in the bulk material sections thereby making it difficult to assess integrity from standard material tests. An accurate appraisal of structural integrity depends primarily on proper assessment of the structural response of the connections and interfaces, and a sound estimate of the loads that induce failure. Accordingly, one must perform a thorough

investigation into the mechanics of the connections and interfaces of the vessel. In addition, real time monitoring of connection integrity is an equally important challenge.

The bolted joint is one of the most common mechanical connections in engineered structures. Often, bolted joints are critical to the function of the structure and their failure may have high associated replacement costs, or may endanger lives. The United States Navy has particular interest in detecting degradation of bolted composite/metal connections due to bolt loosening, because of their current research in developing composite hull forms through MACH and other projects.

1.1 Background on Use of Smart Structural Monitoring Systems

Smart structures are systems in which actuators, sensors and controls have been integrated with structures for functionality. A special class of smart structures which can lead to a completely automated system is obtained by integrating piezoelectric materials with structural systems. This type of approach has found widespread use in engineering applications for self vibration suppression and health monitoring. Piezoelectricity is a phenomenon observed in certain crystals, e.g., quartz, PZT (Lead Zirconate Titanate) ceramic materials and PVDF (polyvinylidene fluoride) polymer. In the direct piezoelectric effect, a piezoelectric material generates an electric field when subjected to a mechanical strain. In the converse piezoelectric effect, the piezoelectric material exhibits mechanical deformation when subjected to an electric field. This coupling between electrical and mechanical energy makes piezoelectric materials very useful in many applications as transducers or as actuators.

More than a decade of intensive research in the area of smart materials and structures has demonstrated the viability and potential of this technology. Numerous applications have been proposed and conceived experimentally for piezoelectric smart structures, such as for active vibration suppression, noise cancellation, shape control and structural health monitoring. By bonding piezoelectric actuators to a structure at desired locations as actuators, dynamic strain can be induced in a prescribed waveform by applying appropriate voltages to the actuators. This can be used to dynamically excite a structure in a controlled manner for integrity interrogation. Piezoelectric materials bonded to structures can also be used as dynamic strain sensors. It should be noted that piezoelectric

sensors measure dynamic strain only, since piezoelectric materials are capacitive in nature and cannot measure continuous static strain. While static strain will cause an initial output, this signal will slowly decay based on the piezoelectric material and time constant of the attached electronics.

1.2 Objectives

The objective of this study is to determine the effectiveness of different vibration-based techniques for the detection of stress relaxation in bolted hybrid connections. A method capable of determining the severity of the stress relaxation is the primary goal. Furthermore, techniques to ascertain the location where the bolt load has relaxed is also desired. The United States Navy has particular interest in detecting degradation of bolted composite connections due to bolt loosening because of their current research in developing hybrid composite/metal hull forms. The U.S. Navy currently has a technical goal to develop systems that use more composite materials. One item of concern for the U.S. Navy is bolted connections that loosen with time due to creep in the composite, dynamic loading or other environmental effects.

1.3 Scope of Work

The focus of this report is a summary of an experimental investigation into various vibration based structural health-monitoring techniques for detecting stress relaxation in bolted composite hybrid connections. Section 2 begins with a literature review of previous work in the field of structural health monitoring using vibration techniques. The mathematical theories and experimental methods employed are also presented in this section. An experimental investigation, performed at the University of Maine, of selected methods is presented in Section 3 and the test results are described in Section 4. These methods include the use of low frequency vibrations, transfer functions and the transmittance function techniques. The report is concluded with a discussion of the results and relative performance of the selected structural-health monitoring techniques.

2. MONITORING TECHNIQUES FOR STRESS RELAXATION

This section presents a literature review of previous work in the field of structural health monitoring using vibration techniques. Several methods that are applicable to detection of stress relaxation in bolted hybrid connections are selected and detailed. In particular, methods using transfer functions and transmittance functions to detect changes are focused upon. The theoretical basis of these techniques, as applicable to this investigation, is described.

The development of structural health monitoring and damage detection schemes has been the focus of much research, especially for the health monitoring of composite structures. Composite materials are used increasingly in engineering applications because of their high specific stiffness and strength. However, they are susceptible to many types of damage such as matrix cracking, fiber breakage or pullout and delamination. Hybrid composite/metal joints in particular are susceptible to fatigue, bolt loosening due to creep, temperature effects and moisture absorption. There are numerous structural health monitoring techniques currently available for detection of structural damage. However, there has not been much research on the structural health monitoring of bolt stress relaxation. Techniques developed from other methods reported in the literature may be applicable to this problem.

The fundamental premise behind vibration-based damage detection techniques is that changes in the physical properties of a system will alter a system's modal properties. Thus changes in mass, damping, and stiffness of a system should lead to measurable changes in the system's dynamic properties, such as the natural frequencies, mode shapes and damping. Comprehensive literature reviews on the subject of structural health monitoring can be found in references Doebling et al. (1996), Farrar et al. (1997) and Zou et al. (2000). Three of the major structural health monitoring techniques discussed here are techniques using impedance sensors, transfer functions and transmittance functions.

The use of statistical analysis procedure was applied to a vibration based damage detection scheme by Fugate et al. (2001). Statistical pattern recognition is applied to the problem of damage detection in this paper. This method relies on measuring a healthy system's characteristics first, and then generating errors as the system's characteristics

deviate when damage occurs. Damage was detected when a statistically significant number of error terms occurred outside a determined control limit.

A passive control technique using piezoelectric materials was used to detect damage (Lew and Juang, 2002). In this method, the natural frequencies of a system are identified to detect damage in a closed loop system, and stability is ensured. A system's damping almost always increases when a virtual passive controller is added.

Techniques based on neural networks require a model to "train" the system to be able to detect damage (Wang and Huang, 2000). Zubaydi et al. (2002) investigated the damage detection of composite ship hulls using neural networks. They developed a Finite Element model for a stiffened plate to simulate dynamic response of the structure with and without damage. They were successful in identifying crack length and location on a faceplate.

Very small damages in composite materials, such as cracks, were successfully found using wavelet analysis (Yan and Yam, 2002). They used a Finite Element model and micro-mechanics theory of composite damage. A crack size as small as 0.06% of the total plate area can be efficiently detected using the wavelet analysis technique.

An interesting method of detecting damage was presented by Todd et al. (2001) using a state-space method. A novel feature called the *local attractor variance ratio* was presented. The paper showed how, through a chaotic excitation, a robust method was developed to detect structural damage using a state space method.

Localized flexibility matrices properties were the focus of the model-based structural damage detection investigated by Park et al. (1998). The three flexibility methods investigated were; a free-free sub-structural flexibility method, a deformation-based flexibility method, and a strain-based flexibility method. The structural damage detection methods were based on the relative changes in localized flexibility.

Often damage detection schemes are first proven theoretically and then investigated experimentally. Kim and Stubbs (2002) presented one such paper, where they used a finite element analysis package (ABAQUS, 2002) to evaluate a two-span continuous beam with modeled damage. A derived algorithm was used to predict the locations and

severities of damage using changes in modal characteristics (Kim and Stubbs, 2002). Banks and Emeric (1998) used a Galerkin method to approximate the dynamic response of structures with piezoelectric patches acting as sensors and actuators. Non-symmetrical damage such as a cut that extended part of the way into a beam was investigated. The analytical results compared well with experimental results in the range of investigation up to 1000 Hz.

Ganguli (2001) used a fuzzy logic system to locate damage on helicopter rotor blades. A fuzzy logic system can be expressed as a linear combination of fuzzy basis function and is a universal function approximator (Ganguli, 2001). The purpose of this study was to determine the approximate location of the damage and then allow for other more intrusive techniques to pinpoint the damage location.

2.1 Damage Detection through Changes in Natural Frequencies

Salawu (1997) has presented an excellent review of various investigations on the effects of structural damage on natural frequencies. Many damage location methods use changes in resonant frequencies because frequency measurements can be quickly conducted and are often reliable. However changes in ambient conditions such as temperature can cause significant frequency changes in composite materials, and findings suggest that detection of damage using frequency measurements might be unreliable when the damage is located at regions of low stress (Salawu, 1997). Similar results were presented by Kessler et al. (2002) where the frequency response method was found to be reliable for detecting damage in simple composite structures, but information about damage type, size, location and orientation could not be obtained. Another investigation by Zak et al. (2000) showed good agreement between experimental and numerical calculations of the first three bending natural frequencies of a delaminated composite beam. Kuo and Jayasuriya (2002) used transfer functions to determine the extent of joint loosening in automobile vehicle frames with high mileage. The method was successful as presented in the paper, but did not give specifics for frequency ranges investigated and what type of frequency response functions were utilized.

2.2 Impedance Based Methods

Impedance-based structural health monitoring techniques show much promise, but require some rather expensive hardware. The impedance-based technique utilizes the direct and converse electromechanical properties of piezoelectric materials, which allows for simultaneous actuation and sensing. The fundamental principle is to track the high frequency (typically > 30 kHz) electrical point impedance of a piezoelectric material bonded onto a structure (Park et al., 2000). A change in the structural mechanical impedance is caused by physical changes in the structure, which induces a change in the electrical impedance of the piezoelectric material, because of the electromechanical coupling between the piezoelectric material and the structure. Thus, structural damage can be identified by monitoring the changes in electrical impedance of the piezoelectric material. This technique is very sensitive at high frequencies because the wavelength of the excitation is small enough to detect incipient-type damage like slight delaminations or loose joints (Kabeya, 1998). Some problems associated with the electrical impedance methods are that the material properties of both the piezoelectric material and composite structures are temperature dependant, so temperature variation can be interpreted as damage. A frequency range of 70kHz to 80kHz was used by Kabeya (1998). Since the excitation frequencies are very high, the piezoelectric sensors are limited in their sensing areas and a large number of piezoelectric sensors and actuators are required to adequately cover the structure. Moreover, since this technique only uses point measurements of the electrical impedance of sensors and does not use mutual information between them, the ability to identify damage location is poor. One major benefit of the impedance method is that it is not based on a theoretical model, as were most other techniques presented earlier, and thus can be applied to complex structures. The application of impedance based monitoring techniques was presented by Berman et al. (1999) for the fiber reinforcement of masonry structures.

2.3 Transfer Functions

Transfer functions characterize the dynamic properties of a system. Transfer functions are measured dynamically by initiating a system response with some type of forcing function, and measuring the resulting system output. In vibration measurements the

output that can be measured are displacement, velocity, or acceleration. A transfer function of a system is a measure of the system's response to a given input excitation. The equation of motion of a single degree-of-freedom system consisting of a spring, mass and damper subjected to an excitation force is

$$m\frac{d^2x}{dt^2}+c\frac{dx}{dt}+kx=F(t) \tag{2.1}$$

The Laplace transform of the system's equation of motion equation (2.1) for system under forced excitation is the transfer function *H*. The Laplace transform converts equation (2.1) from the time domain to the frequency domain. The corresponding Laplace transform of the equation of motion is given in equation (2.2).

$$H(j\omega)=\frac{X(j\omega)}{F(j\omega)}=\frac{1}{m(j\omega)^2+c(j\omega)+k} \tag{2.2}$$

Transfer functions are excellent tools for determining a system's natural frequencies. When the driving frequency equals the undamped natural frequency, the system's response peaks, because of the following condition $k-m\omega^2=0$. This allows the natural frequencies to be determined from a plot of the transfer function magnitude versus forcing frequency. For higher-order systems with multiple natural frequencies, the resonant frequencies correspond to the plots peaks, as can be seen by the representative transfer function in Figure 2-1, and in this example the first three peaks correspond to frequencies of 1050 Hz, 1650 Hz, and 2400 Hz, respectively.

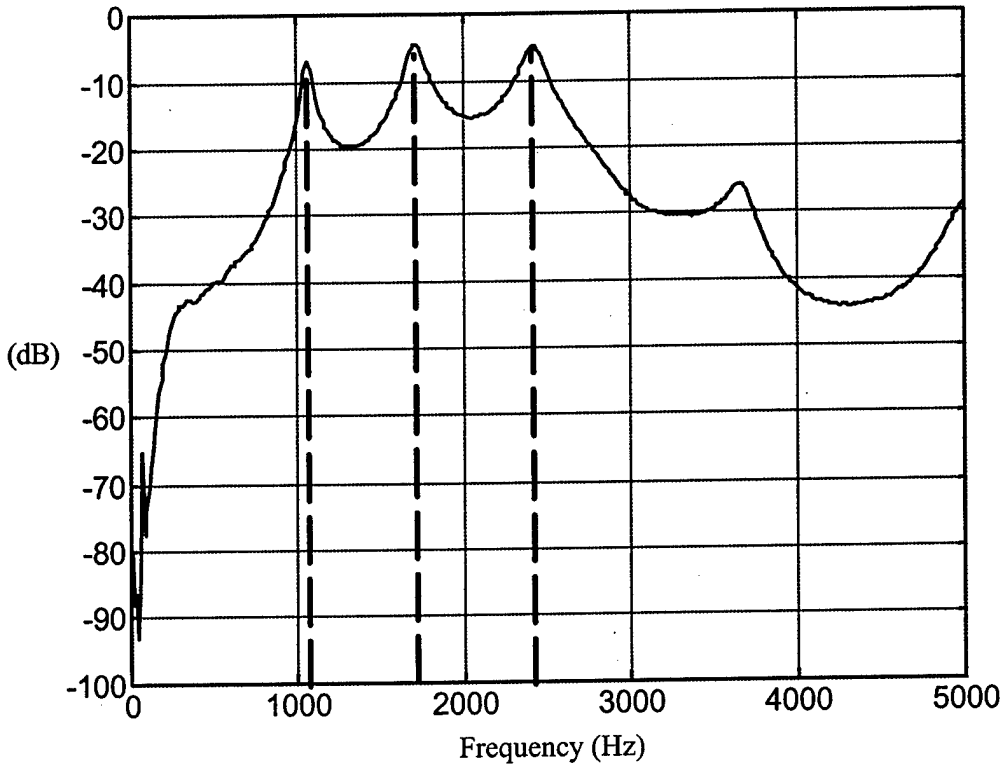

Figure 2.1 - Representative Transfer Function

Experimental measurement of the transfer function of continuous systems is not as simple as taking the Laplace transform of the equation of motion as illustrated earlier. The mass, stiffness, and damping matrices can be estimated, but not calculated exactly for most real continuous systems. Thus, the responses measured by the transducers are discretized in order to take advantage of existing computational power. Discretization of the data, and noise in the system, prohibits the data to be analyzed in a deterministic fashion as shown earlier. Presented subsequently is the method used to estimate the transfer function of a system.

For a discrete signal, the position, velocity, or acceleration relative to time can be measured. A measure of how fast that signal is changing with time is the autocorrelation function given by Equation (2.3). Likewise a measure of how one signal $x(t)$ is changing relative to another signal $f(t)$ is the cross-correlation of the signals given by equation (2.4). Here $x(t)$ is the response of the system, and $f(t)$ is the forcing function.

$$R_{xx} = \lim_{T \to \infty} \frac{1}{T} \int_0^T x(t)x(t+\tau)dt \tag{2.3}$$

$$R_{xf} = \lim_{T \to \infty} \frac{1}{T} \int_0^T x(t)f(t+\tau)dt \tag{2.4}$$

The autocorrelation and cross-correlation is then converted to the frequency domain by employing the discrete Fourier transform. The spectral density is the discrete Fourier transform of the autocorrelation, and likewise, the cross-spectral density is the discrete Fourier transform of the cross-correlation. Equations (2.5) and (2.6) are the spectral density and cross-spectral density respectively.

$$S_{xx}(\omega) = \frac{1}{2\pi} \int_{-\infty}^{\infty} R_{xx}(\tau)e^{-j\omega\tau}d\tau \tag{2.5}$$

$$S_{xf}(\omega) = \frac{1}{2\pi} \int_{-\infty}^{\infty} R_{xf}(\tau)e^{-j\omega\tau}d\tau \tag{2.6}$$

The spectral and cross-spectral densities can be used to compute the transfer function of a system as shown by the spectral densities relationship equations (2.7) and (2.8) given below. A development of equations (2.7) and (2.8) is described by Inman (2000). The signal processing hardware used to estimate the transfer functions employs these equations in its estimation of the transfer function. $S_{xx}(\omega)$ is the spectral density of the response, and $S_{xf}(\omega)$ is the cross-spectral density of the response with respect to the forcing function $f(t)$. Likewise, $S_{fx}(\omega)$ is the cross-spectral density of the forcing function with respect to the response $x(t)$, and $S_{ff}(\omega)$ is the spectral density of the forcing function.

$$S_{xx}(\omega) = H(j\omega)S_{xf}(\omega) \tag{2.7}$$

$$S_{fx}(\omega) = H(j\omega)S_{ff}(\omega) \tag{2.8}$$

The coherence function (equation 2.9) is used as a measure of the quality of data gathered using the spectral densities. The coherence function can only range from zero to one, with one meaning that the transfer functions obtain by equations (2.7) and (2.8) are

equal. A coherence of unity indicates that the two transfer function estimates are correlated. If the coherence equals zero, then the two transfer functions are uncorrelated and the signal is pure noise.

$$\gamma^2 = \frac{\left|S_{xf}(\omega)\right|^2}{S_{xx}(\omega)S_{ff}(\omega)} \tag{2.9}$$

2.4 Transmittance Functions

Transmittance functions (TF) are derived as the complex ratio between Fourier transforms of a response point and a reference point on a structure. The motivation for using the TF is that excitation does not need to be measured, therefore, changes in the structure due to the environmental effects (temperature and moisture) are partly cancelled. Also, the cross-spectral density used in TF is a measure of the linearity between two response points on the structure and can detect local damage by propagation changes (phase delay and amplitude modulation) in the structural response. Since the cross-spectral density function is the Fourier transform of the cross-correlation function, it represents the frequency domain characterization of the similarity of the magnitude and phase of two signals, e.g. of two nearby response points on the structure. Hence, if used in the correct frequency range, it can accurately detect damage over small distances on a structure. Furthermore, measured transmittance data inherit certain advantages over modal data. Firstly, transmittance functions have few sources for computing error, except the minimal error from the numerical Fast Fourier Transform. Secondly, they carry complete information on the dynamic behavior of the test structure, in terms of both the vibration modes and the damping, at many frequency points, including those away from the response of the structure (Zhang et al., 1999).

The transmittance function does not depend on whether the receptance, mobility or inertance spectral densities are measured, since it is a ratio of the frequency response functions. Therefore, different sensor types can be used to measure the vibration response. When damage occurs, the peaks and valleys of the transmittance function misalign. This misalignment caused by a change between the healthy and damaged system can be quantified. Generally, the sensitivity of the technique to detect small

damage increases as the actuator and sensor move close to the damage, and as the frequency of excitation increases (Schulz et al., 1999). The damage values for some cases are nearly four times larger at high frequencies (10-20 kHz) than at low frequencies (200-1800 Hz) (Zhang et al., 1999). However, the size of the PZT sensors plays a role in the effective frequency range over which the sensor can detect damage. Different sized sensors are more tuned for certain vibration frequencies. A larger sensor would not be as effective as a small sensor for detecting high frequency vibration, because the sensor would be much larger than the vibration wavelengths. Also, at the higher frequencies there are additional hardware concerns, because of the higher sampling rate and the likelihood that additional sensors will be required.

Advantages of transmittance functions as stated by Schulz et al. (1997) are as follows:

1. No structural model is needed.
2. Excitation does not need to be measured.
3. The non-resonant and anti-resonant (zeros) parts of the transmittance functions are very sensitive and can detect small damage (cracks) that other methods miss.
4. Simultaneous multiple damages can be detected.
5. Well developed sensor and signal processing techniques are used rather than unproven impedance methods.
6. Transmittance functions are highly repeatable diagnostic procedures, because environmentally induced changes in the physical properties of the structure are mostly cancelled by the ratio of response quantities in the transmittance functions.
7. Transmittance functions have a high dynamic range and can decompose the response signal/noise into different frequency bands to focus on abrupt spectral changes due to damage.
8. Measurement noise tends to be canceled by the normalization in the transmittance function.
9. The transmittance function technique is algorithmically simple and suitable for autonomous damage detection.

Additional tests on other types of structures and damages are needed to confirm the characteristics of this method. Successful transmittance function testing for wind turbine blade damage analysis was presented by Ghoshal et al. (2000) and by Schulz et al. (1999) for beams and plates.

Transmittance functions (TF) characterize the response at two different points of a system for a given input. Transmittance functions are a ratio of the response cross-spectral density between two sensors, and the response auto-spectral density at a point, and it is a non-dimensional complex quantity that defines how vibration is transmitted between two locations as function of frequency. Displacement, velocity, or acceleration measurements can be used to compute the transmittance function. The transmittance functions are found similarly to the transfer functions discussed in Section 2.4. But instead of computing the spectral densities of the forcing function, the spectral density and cross-spectral density are calculated for two separate sensors on a system excited by the same input. The transmittance function of sensor A with respect to sensor B is defined as

$$T_{ab}(\omega) = \frac{S_{ab}(\omega)}{S_{bb}(\omega)} \tag{2.10}$$

whereas the transmittance function of sensor B with respect to sensor A is defined by

$$T_{ba}(\omega) = \frac{S_{ba}(\omega)}{S_{aa}(\omega)} \tag{2.11}$$

The forcing function does not need to be measured, as long as the measurements at the two different sensors are taken simultaneously to calculate the spectral and cross-spectral densities. The transmittance function estimation is mathematically the same as a transfer function estimation, with the difference being transfer functions are measures of a response to an input, while transmittance functions are measures of a response to another response.

3. EXPERIMENTAL EVALUATION OF BOLT LOOSENING DETECTION METHODS

An experimental platform was created for investigation of the various health-monitoring schemes that showed potential for bolt stress relaxation evaluation of bolted hybrid composite/metal systems. As a test bed, a composite plate to metal frame apparatus was designed and fabricated. The configuration employed is a 24.5-inch square Eglass/vinyl ester composite plate bolted to a steel frame with sixteen ½-inch diameter grade eight steel bolts. This experimental setup is described in detail in this section of the report.

3.1 Fiberglass Plate Configuration

The ¼ inch thick fiberglass plate used in the following experiments consisted of eight layers of Brunswick Technologies Inc. 0/90 Eglass knit fabric (BTI CM-2408) in a symmetric lay-up, $[(0/90)_4]_S$. The matrix material is a Dow Derakane 8084 resin infused at the University of Maine Crosby Laboratory, using a Vacuum Assisted Resin Transfer Molding (VARTM) process. The test panel was wet-saw cut from a larger panel (UMCL-35, 48 inches by 30 inches by ¼-inch thick) to a dimension of 24.5-inch square. Sixteen 9/16 inch holes were drilled around the plate perimeter so that it could be bolted to a steel picture frame base. A 9/16-inch diamond coated drill bit, supplied by Accurate Diamond Tool Corporation of Emerson, New Jersey, was used to drill the holes. The bolt pattern used for the composite plate matches with the bolt pattern for the steel frame. Figure 3.1 depicts the steel frame that was fabricated by Alexander's Welding and Machine of Greenfield, Maine. The larger 9/16-inch holes are for the ½ inch grade eight bolts that attach the fiberglass plate to the frame. The smaller counter-sunk holes are for the ¼ inch bolts, which attach the frame to the laboratory worktable. The worktable has a ¼ diameter bolt pattern spaced two inches on center. Wooden blocks were used as spacers to support the plate above the table to facilitate access to the bottom of the frame for tightening and loosening the ½ inch steel bolts.

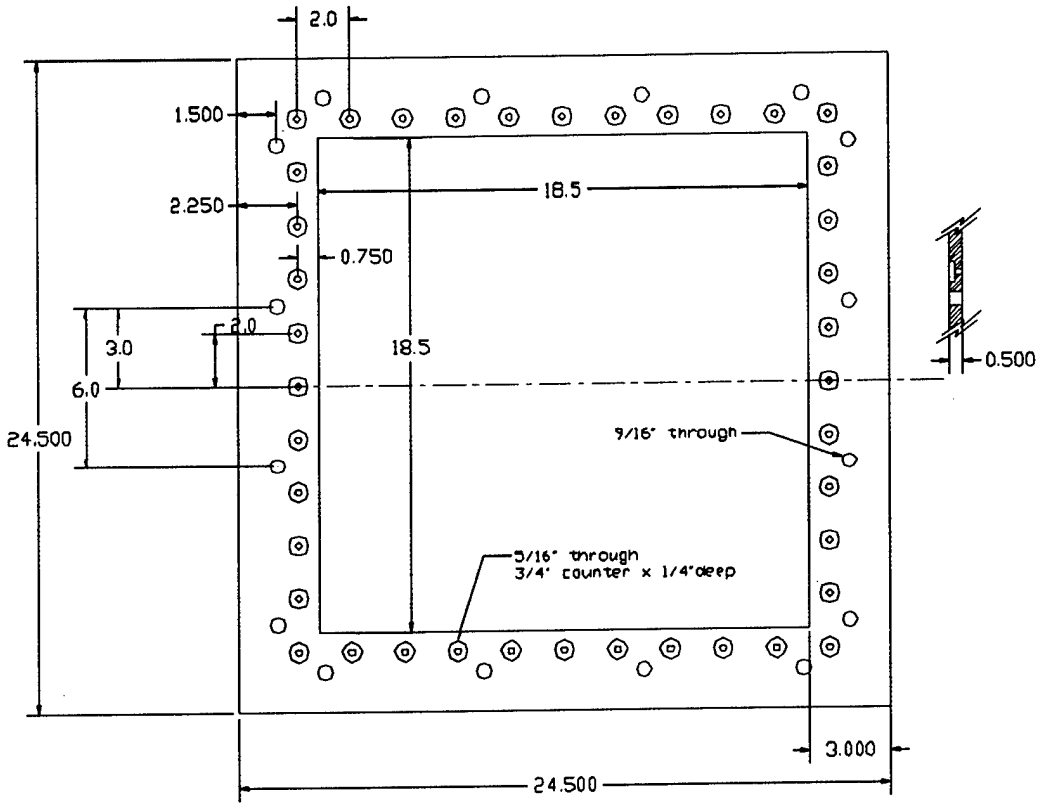

Figure 3.1 - Steel Frame Schematic with Dimensions in Inches

The grade eight bolts used to fasten the plate were supplied by A.L. Design Inc. of Buffalo, New York. The bolts were ½ inch diameter by 2 inches long with 1.5 inches of thread. For the experiments, one of the bolts was internally gauged with strain gauges. This instrumented load-sensing bolt (model ALD-BOLT-1/2-2, serial # 220807) was identical to the other bolts, except for the internal strain gauges. The full-bridge strain gauge configuration, in the load bolt, was excited by 10 V DC, and the output voltage (in mV) was correlated to the bolt load.

The complete calibration sheet for ALD-BOLT-1/2-2, serial # 220807, can be found in Appendix A. Figure 3.2 shows an instrumented bolt configuration. The fiberglass plate is on top of the steel frame with the wooden spacer blocks supporting the frame above the table.

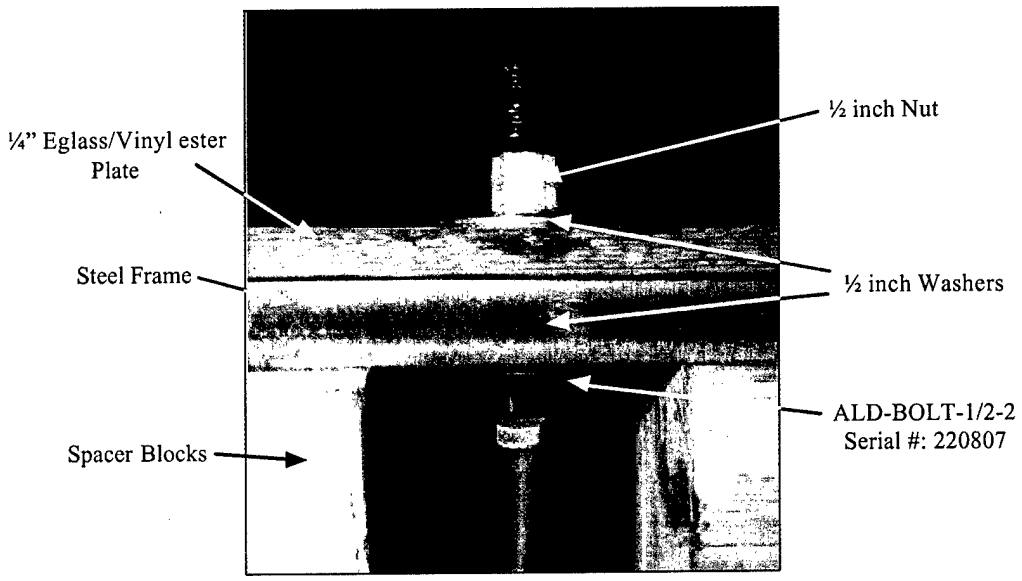

Figure 3.2 - Instrumented Bolt Configuration.

3.1.1 Dynamic Sensors and Actuators

A piezoelectric actuator (ACX QP 10W) was bonded to the center of the plate by applying an epoxy adhesive between the actuator and plate and vacuum bagging it for three hours minimum. Figure 3.3 shows the setup with the actuator bonded at the center of the plate, and sensors for the high frequency tests located near two of the bolts. Complete specifications of the ACX piezoelectric actuator are given in Appendix C. ACX actuators were chosen because of their slim, low-profile design, and they came with the wire leads already attached to the piezoelectric wafers. Early in the investigation soldering wire leads to piezoelectric wafers was experimented with, but this proved to be cumbersome.

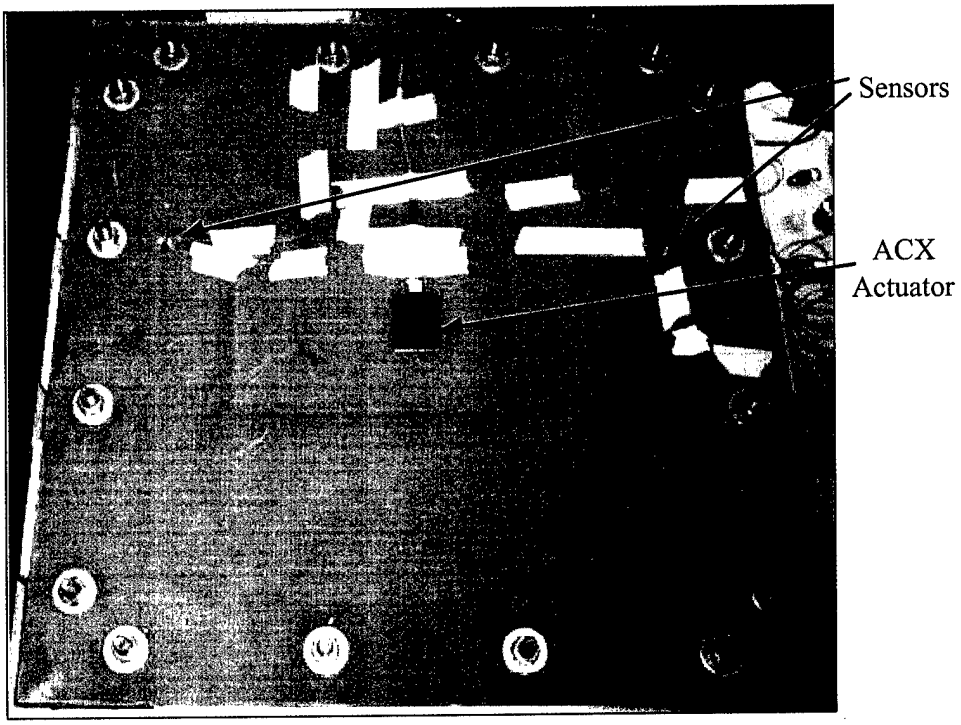

Figure 3.3 - Sensors and Actuators Mounted on the Plate

Accelerometers and dynamic strain sensors were used to measure the response of the plate to an excitation. An accelerometer and a dynamic strain sensor used in these experiments are depicted in Figure 3-4. The accelerometer senses acceleration transverse to the plane of the plate, while the strain sensor measures the in-plane dynamic strain induced in the plate from the vibration. Both sensors were supplied by PCB Piezotronics of Depew, New York. Model 352B10 ceramic shear ICP accelerometers were chosen for their ability to measure low amplitude vibration, minimal mass, and ability to operate in a frequency range of up to 25 kHz. ICP is a trademark of PCB, and sensors with this designation have internal signal conditioning circuitry that minimizes noise and improves sensor accuracy. Complete specifications for model 352B10 accelerometers are given in Appendix D. The dynamic strain sensor, model 740B02, was chosen for its low profile, and because it is less expensive than an accelerometer of the same capability. Because of cost considerations strain sensors are an attractive option for large-scale health monitoring schemes. Complete dynamic strain sensor specifications can be found in Appendix D. For the lower frequency dynamic measurements a model 352A24 PCB

accelerometer was used. This accelerometer was used for the early experiments to determine the fundamental frequency before the higher frequency accelerometers were purchased. The reader is referred to Appendix D for specifications.

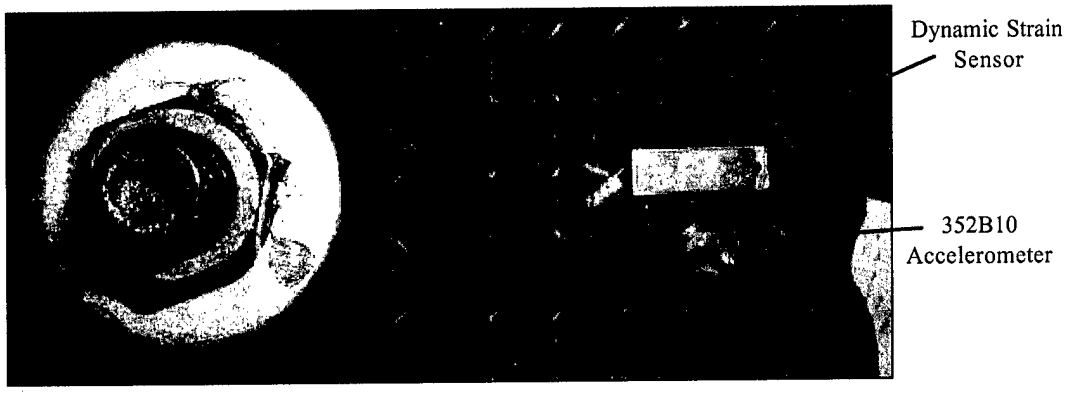

Figure 3.4 - Dynamic Strain Sensor and Accelerometer

3.1.2 Electronics

Various electronic components were employed to complete the experimental setup. Voltage sources and measurement devices were used with the sensors, and a sophisticated data acquisition system completed the setup. The instrumented bolts were excited, per specifications, by a Hewlett Packard 3245A Universal Source (serial # 2831A02484) set to 10 volts DC, and a Micronta Auto-Range Digital Multimeter (serial # 22-195S) was used to read the output voltage. The ACX actuator's excitation signal was generated by a SigLab module and amplified by a PCB 790A01 signal conditioner (serial # 274) with a set gain of 25. PCB accelerometers and dynamic strain sensors signals were conditioned by a 482A20 PCB ICP sensor signal conditioner. The signal conditioner was set to unity gain for the accelerometers. However, the strain sensor's lower output required a gain of ten for the lower frequency ranges, and a gain of unity at frequencies over 1-kHz. The excitation signal was generated using a SigLab dynamic signal acquisition and processing hardware. SigLab is a dynamic signal and system analyzer that runs on a MATLAB platform with function generation, spectrum analyzer, oscilloscope, and network analyzer capabilities. The SigLab hardware has two input and two output channels, as shown in Figure 3.5, and a bandwidth of 20 kHz. SigLab is used

as the function generator, data acquisition system, and data analyzer in the experiments. Hardware specifications for the PCB signal conditioner, and SigLab is presented in Appendix E and Appendix B, respectively.

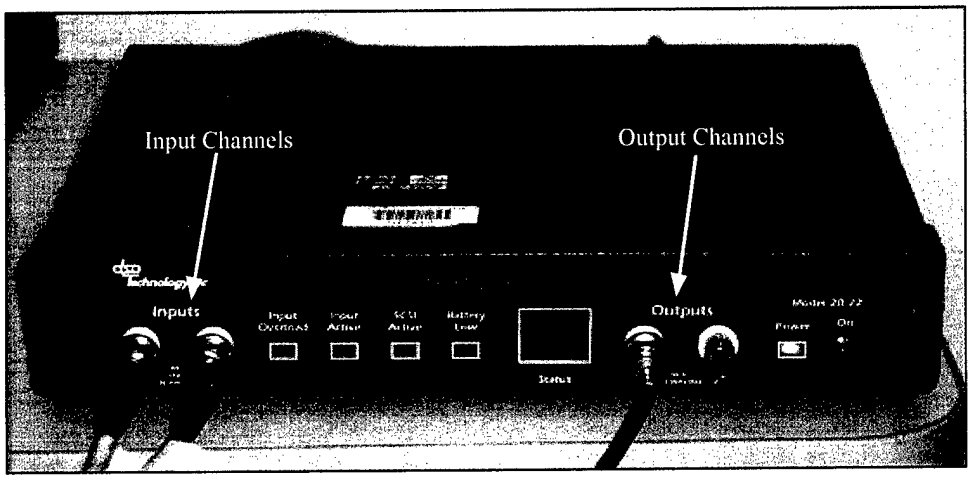

Figure 3.5 - SigLab Hardware

3.2 Experimental Procedure

The experimental procedures followed in conducting the various studies are described in detail in this section. Test results, data reduction and analysis are summarized in Section 4.

3.2.1 Bolt Torque Repeatability

Bolt torque repeatability experiments were conducted to determine how reliable a calibrated torque wrench was at applying the desired tensile loads in the bolts. Although it was desirable to know the force in each of the bolts, it was prohibitively expensive to use instrumented bolts for all 16 bolts around the perimeter of the plate. Therefore, it was necessary to correlate the applied torque to the bolt load.

In this experiment, the torque of the instrumented bolt was varied, while the other bolts were maintained at constant torque sufficient to prevent any plate movement. The instrumented bolt was lubricated with Loctite Anti-Seize and threaded through the bolt hole with the nut on the top of the plate, as shown in Figure 3-2. The Anti-Seize acts as a

bolt lubricant and thus the torque to load estimation should be more reliable. The HP power source was then connected to the appropriate leads on the instrumented bolt and set to 10 volts DC. A Micronta multimeter was also turned on, and connected to the instrumented bolt. The electronics were left on for a period of time not less than 20 minutes for each trial before starting the tests. This warm-up period is required to ensure accuracy of the bolt's output, per A. L. Design Inc. information sheet in Appendix A. The bolt was then tightened to 20 foot-lbs by the 10 to 100 foot pound Armstrong torque wrench (serial # 4010486831). After the voltage readout was recorded, the torque was increased by five foot-lbs. increments and the corresponding voltage recorded until the final torque of 50 foot-lbs. The process was repeated six more times for a total of seven trials over the 20 to 50 foot-lbs. range.

3.2.2 Variation of Fundamental Frequency with Uniform Torque

The purpose of the variation of fundamental frequency with uniform bolt torque study is to investigate the effect of the perimeter clamping force on the fundamental frequency of the plate. The 24.5-inch square fiberglass plate is clamped to the steel frame using sixteen ½-inch diameter grade eight bolts. The torques were applied to the bolts using two different Armstrong micrometer torque wrenches. The smaller torque wrench (serial # 960831060) had a torque range of 50 to 250 inch pounds of torque, while the larger wrench was capable of 10 to 100 foot pounds of torque (serial # 4010486831). The response of the plate was sensed by a PCB 352A24 accelerometer mounted 0.75 inches from the edge of the ACX actuator as shown in Figure 3.6.

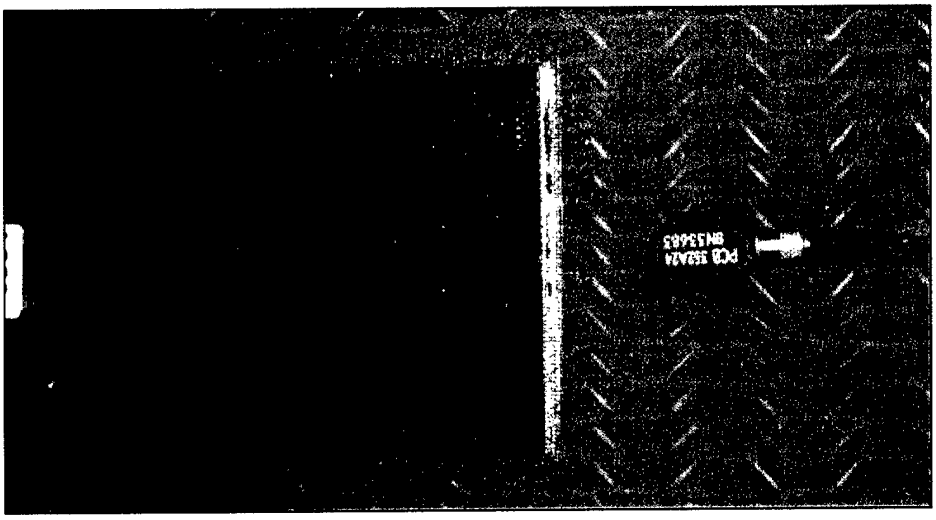

Figure 3.6 - 352A24 Accelerometer Placement Relative to the ACX Actuator

Fifteen regular grade eight bolts were threaded through the plate holes with the sixteenth bolt being the instrumented bolt. All of the bolts were lubricated with Loctite nickel Anti-Seize and the nuts threaded down so that they did not quite touch the washers. After the installation of the plate, the HP function generator and Micronta multimeter were switched on and connected to the instrumented bolt, as were the ACX actuators and PCB accelerometer connected to their respective signal conditioners. The electronics and the SigLab hardware were also turned on and allowed to warm up for a period of at least 20 minutes.

For the first trial, the bolts were left loose enough to rattle in the holes. Siglab's dynamic signal analyzer was set to average the data from three trials consisting of 4096 data points recorded. The system excitation was a two volts root mean square (VRMS) chirp function over a frequency range of 0 to 1000 Hz. Estimation of the transfer function was performed with the network analyzer module (VNA) of the SigLab interface program. The fundamental frequency was estimated from the transfer function. Another experiment with a narrower bandwidth, of 100 Hz around the fundamental frequency, was performed to accurately determine the fundamental frequency. Both transfer functions, the fundamental frequency, and the instrumented bolt voltage were recorded.

Next, the bolts were torqued to 50 inch pounds using the 50 to 250 in-lb torque wrench in the order shown in Figure 3.7. The corresponding transfer function and pertinent data were recorded. The 10 to 100 ft-lbs. torque wrench was used for torques greater than 300 in-lb. During the lower torque trials, the torque was incremented by 10 in-lbs., whereas for higher torques, larger torque increments were used. The following torques were applied to all the bolts: 0, 50, 60, 70, 80, 90, 100, 110, 120, 130, 140, 150, 160, 170, 200, 230, 300, 360, 480, 600 and 720 in-lbs.

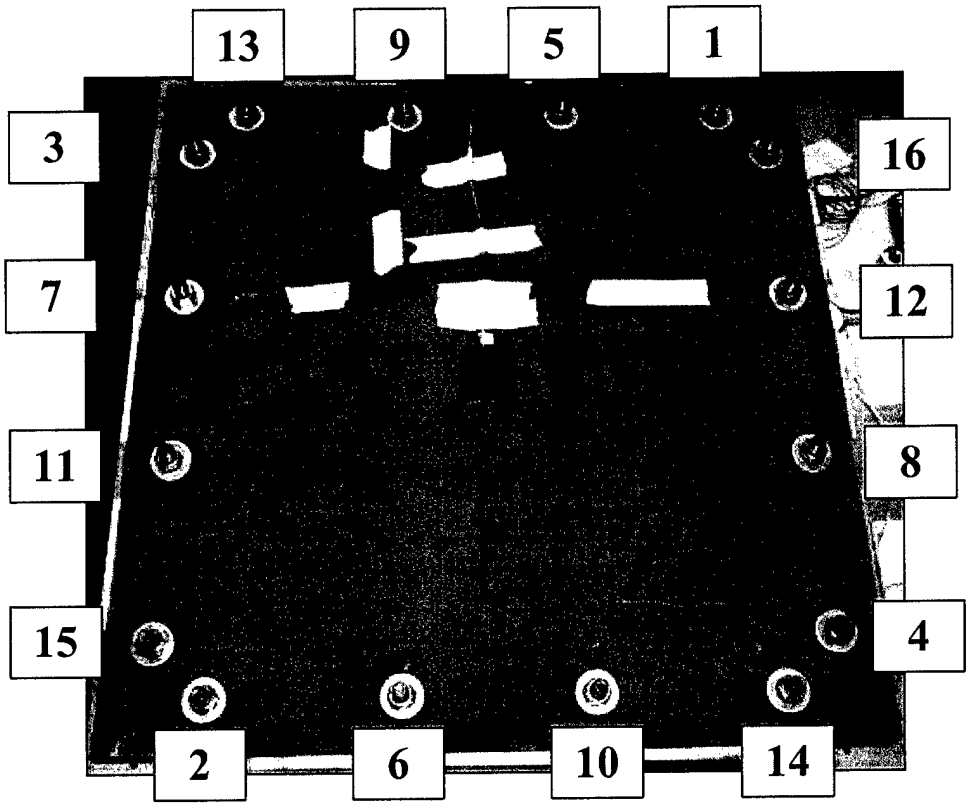

Figure 3.7 - Bolt Torque Pattern

3.2.3 Fundamental Frequency Dependency on Single Bolt

The technique to investigate use of the fundamental frequency to detect loosening of a single bolt is presented in this section. The bolt torque for the single instrumented bolt is changed while keeping the other 15 bolts at a constant value. The experimental procedure is identical to the procedure given in Section 3.2.2, except that only one bolt has the torque varied as opposed to adjusting the torque of all 16 bolts.

For the first trial the 15 non-instrumented bolts were tightened to the full torque load of 720 inch pounds. Siglab's dynamic signal analyzer settings were adjusted as discussed in the experimental setup. The Siglab network analyzer was used to record the transfer function of the plate for a frequency range of 0 to 1000 Hz. The fundamental frequency was picked off the transfer function and a second transfer function was found for a narrower bandwidth of 100 Hz around the fundamental frequency. Both transfer functions outputs were then saved, and the fundamental frequency and the instrumented bolt voltage, were recorded.

The instrumented bolt was loosened, and then tightened to 600 inch pounds using the 10 to 100 foot pound torque wrench. The transfer function was measured, and the corresponding data recorded. The torque was decreased incrementally from 600 inch pounds to finger tight (or 0 inch pounds) in the following steps: 600, 480, 360, 230, 200, 170, 160, 150, 140, 130, 120, 110, 100, 90, 80, 70, 60, 50 and 0 in-lbs.

3.2.4 High Frequency Response Using Transfer Functions

In the high frequency response experiments, the frequency response of two sensors for a frequency range of 13 kHz to 17 kHz were found for each change in torque. The torque of one bolt only was changed throughout the experiment. One sensor was placed directly next to the bolt that had the torque varied and another sensor was placed directly on the other side of the plate. Both accelerometers and dynamic strain sensors were employed to determine which sensor gave better results. Figure 3.8 shows the high frequency experimental configuration with the accelerometers and dynamic strain sensors. The procedure for this section is similar to the procedure given in Section 3.2.3, except for the frequency range investigated, the types of sensors used, and the sensor locations. The

accelerometers and dynamic strain sensors were placed next to both the instrumented bolt, and the bolt directly opposite, as shown in Figure 3.8. Only the instrumented bolt was loosened to conduct the tests. Model 352B10 ceramic shear ICP accelerometers were the accelerometers employed for these tests, as opposed to the 352A24 accelerometer that was used for the lower frequency tests. Siglab hardware generated the chirp excitation function for the ACX actuator, and measured the two separate transfer functions for a frequency range of 13 kHz to 17 kHz. The PCB ICP signal conditioner was set for a gain of unity when using the accelerometers, and a gain of ten when using the dynamic strain sensors. The transfer functions for both sensor locations were saved. The bolt torque was set and varied, for the instrumented bolt, in the same manner as described in Section 3.2.3.

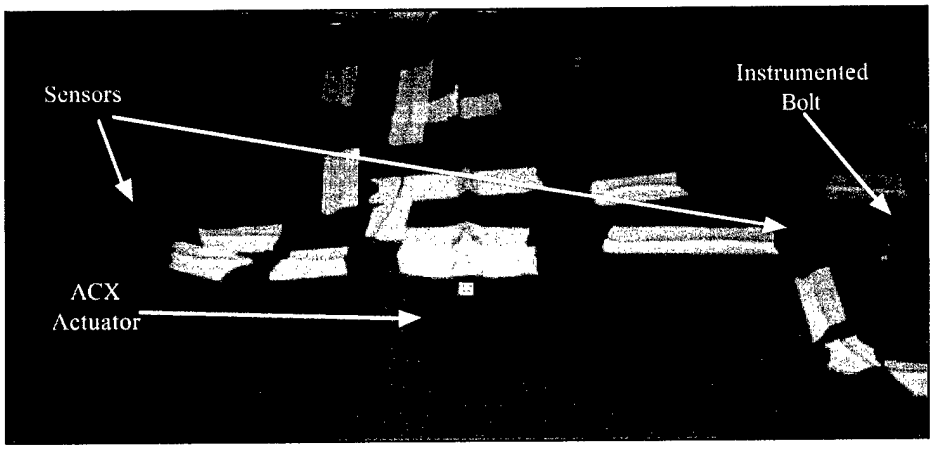

Figure 3.8 - High Frequency Test Configuration

3.3 Transmittance Testing

Transmittance testing procedures are similar to the procedures performed for the transfer function techniques. For the transmittance tests, the response of two sensors are compared to each other, whereas when measuring transfer functions, the response of one sensor is compared with the excitation signal. Thus, for the transmittance testing, sensor A was connected to input channel 1 and sensor B was connected to input channel 2 of the Siglab hardware. Input channel 2 was the reference channel for Siglab, thus the transmittance function A with respect to B (T_{AB}) was calculated using this configuration.

Manhattan switch boxes were used to switch between sensor pairs for each transmittance function to be tested. The switch boxes had four inputs and one output. All four sensors used were connected to each switch box and the corresponding signal of interest was selected by turning the dial as shown in Figure 3.9. The switch boxes were employed to facilitate a quick change of sensors so that multiple transmittance functions could be recorded easily. This continued until all of the desired transmittance functions were found for a given frequency range and level of damage present in the system.

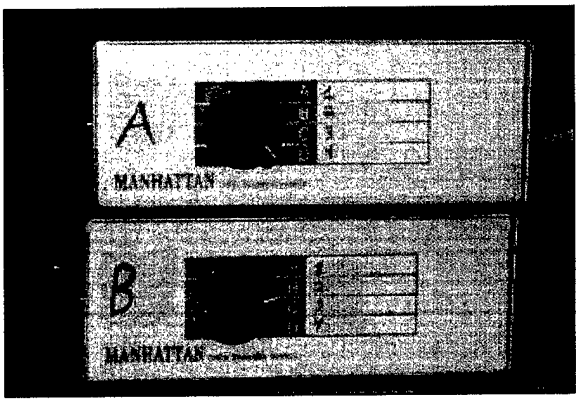

Figure 3.9 - Manhattan Switch Boxes

3.3.1 Frequency Range Investigation

The Siglab dynamic signal analyzer is capable of investigating systems from 0 Hz to 20 kHz, thus this is the absolute limit for the transmittance testing. A frequency bandwidth of 4 kHz was used for the testing in order to give good frequency resolution for the transmittance results. Tests were conducted for the following five frequency ranges in kHz: 0-4, 4-8, 8-12, 12-16, 16-20. An A. L. Designs instrumented bolt was loosened between sensors 2 and 3 for the damage in these series of tests as shown in Figure 3.10. Since the transmittance method was being explored to detect bolt loosening on a composite plate only the transmittance functions T23 and T32 were analyzed in this investigation. Tests were performed per the basic procedure given earlier for all sixteen bolts tightened to 720 in-lbs by the Armstrong 10 to 100 ft-lbs torque wrench. The instrumented bolt indicated in Figure 3.10, was then loosened to 540 in-lbs and the

experiment run again. The bolt was then loosened incrementally from 300 to 60 in-lbs. with the experiment performed at each torque level. For the 60 in- lb case the smaller 50 to 250 in- lb torque wrench was used. The actual tensile load in the bolt was recorded by measuring the output voltage at each step.

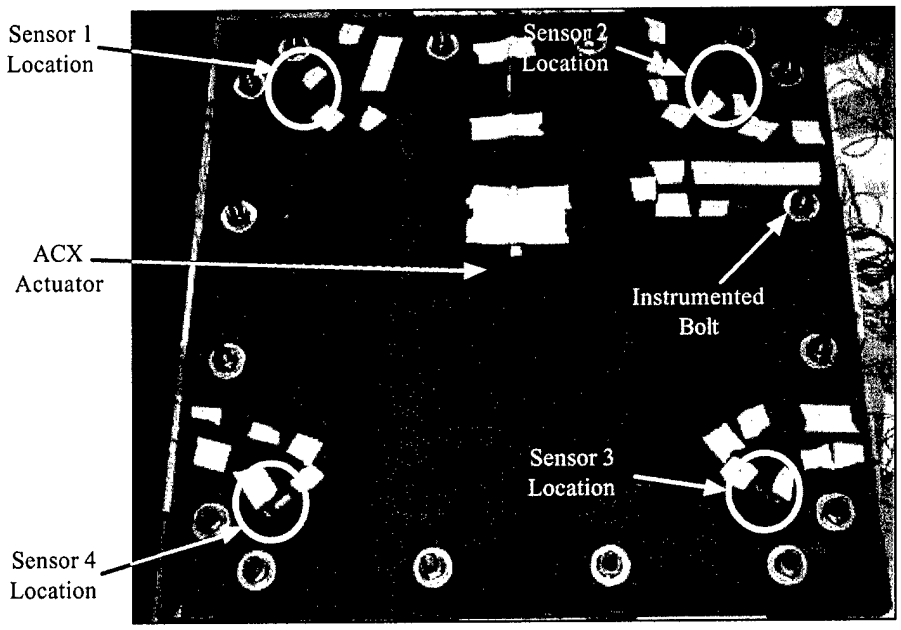

Figure 3.10 - Transmittance Testing Sensor Locations

3.3.2 Transmittance Investigation for One Bolt Loosening

Extensive testing was conducted using the transmittance functions for a single bolt loosening, including a frequency range survey. The two frequency ranges found to produce the best results were used extensively in this series of tests. The same basic transmittance function testing procedures were followed, except tests were conducted for two different frequency ranges simultaneously. A test was conducted for the 7 kHz to 9 kHz range, and at the 18 kHz to 20 kHz range. The bolt torque levels, for the loosened instrumented bolt used in this part of the experiment, were 720, 660, 600, 540, 480, 420, 360, 300, 240, 180, 120, and 60 inch-pounds. The bolt torque was adjusted using the Armstrong 10 to 100 ft-lb torque wrench, for all of the adjustments except for the 120 and 60 in-lb settings that were done with the 50 to 250 in-lb torque wrench. A complete set of transmittance tests were conducted for each torque setting and frequency range.

The transmittance tests were conducted for the following sensors pairs: 12, 21, 23, 32, 34, 43, 41, 14, 13, 31, 24, and 42. The output voltage of the instrumented bolt was recorded for each test. The tests were conducted using both accelerometers and dynamic strain sensors.

3.3.3 Repeatability Procedures

The repeatability of the transmittance test results was investigated by following procedures similar to those described in Section 3.3.2. After initial torquing of all the bolts to 720 in-lbs. the panel was let sit for a period of 2 days. A baseline "healthy" set of data was then recorded. The "healthy" test was not immediately conducted to allow the initial composite creep to subside. This was done in an attempt to limit the effects of creep during the experiment. The loosened bolt torque was reduced to 240 in-lbs. The transmittance functions were recorded between the following sensor pairs: 12, 21, 23, 32, 34, 43, 41, and 14. And the tests were conducted approximately 5 to 10 minutes after the reduced bolt torque was set. The test was repeated several times by completely loosening the bolt and retorquing to 240 in-lbs. The start time of each test was recorded, as was the instrumented bolt voltage, for each test. Ten simulated bolt relaxation cases were conducted.

3.3.4 Bolt Loosening Test Procedures

The procedure to investigate the effects of loosening a different bolt was identical to the extensive transmittance testing procedure, except for: only the accelerometers were used in the 7 kHz to 9 kHz range, a different bolt was loosened, and the following reduced set of bolt torques were investigated, 720, 600, 480, 360, 240, and 120 in-lb. The effects of damage located elsewhere on the plate is investigated here. The bolt loosened for this experiment is on the left side of Figure 3.11.

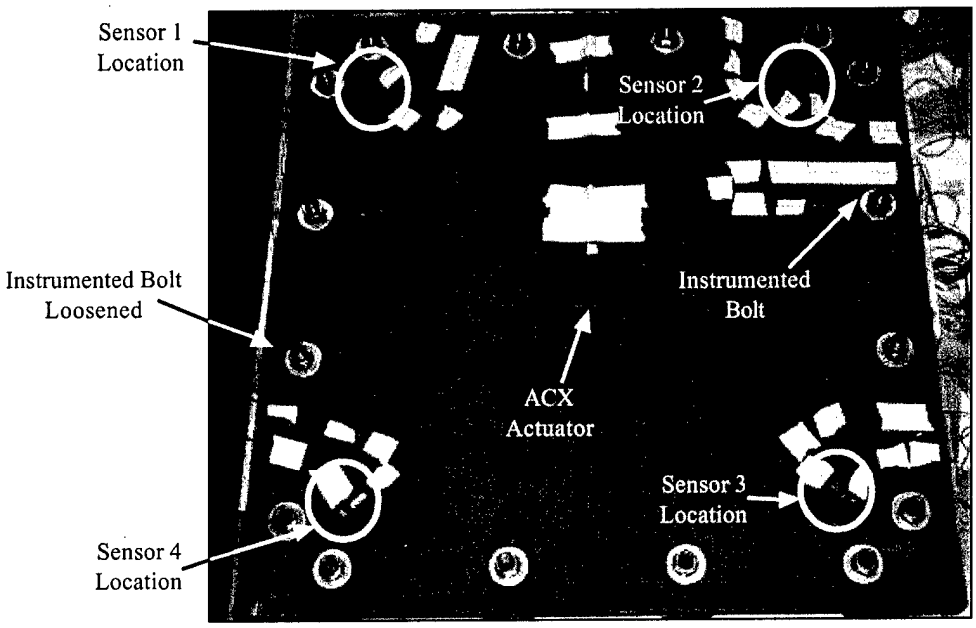

Figure 3.11 - Different Damage Locations

4. SUMMARY OF TEST RESULTS AND DISCUSSION

4.1 Bolt Torque versus Bolt Load Repeatability

The relationship measured between bolt load and bolt torque is described in this section. This was done as a precursor to the bolt loosening studies. This relationship is important in this study because only one instrumented bolt is used per panel and bolt loads are estimated in non-instrumented bolts through this relationship. The repeatability of applying a measured torque with the Armstrong micrometer torque wrench and using this torque to predict bolt load is described. The calibration plot for the instrumented ALD-BOLT-1/2-2 serial number 220807 is presented in Figure 4.1. It shows the relationship of the bolt load to the voltage output, and the corresponding linear equation is given on the plot where Y is the bolt load in pounds and X is the transducer output in mV.

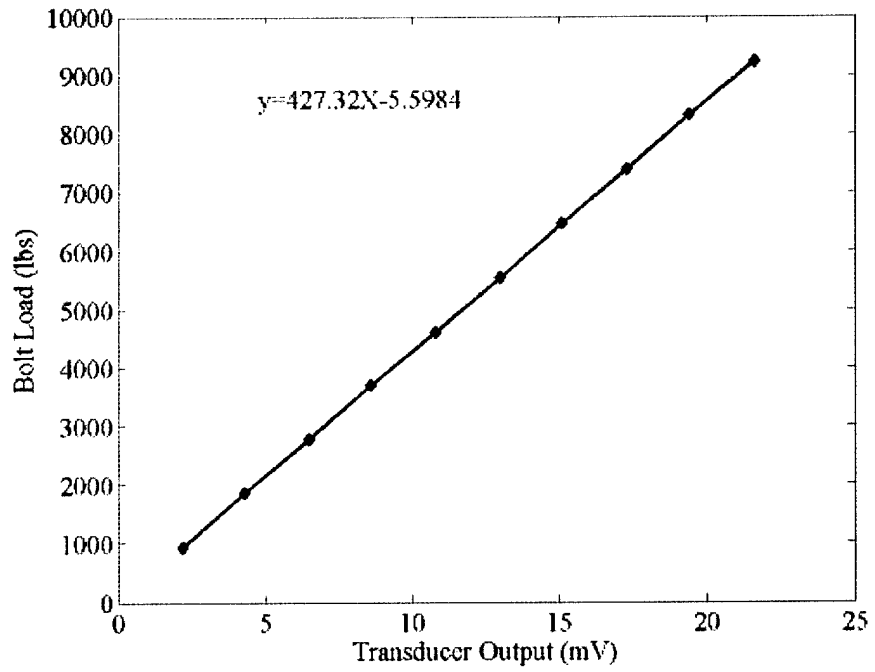

Figure 4.1 - Instrumented Bolt Calibration Chart

Several trials of bolt load versus torque were quantified. The instrumented bolt was lubricated using Locktite anti-seize and the bolt was torqued with an Armstrong torque wrench. Voltage from the bolt was converted to load using the equation in Figure 4.1. For each of seven trials, the output voltage was averaged for each applied torque. Table 4.1 reports the bolt load at various torque values for each trial. Table 4.2 shows the statistical properties of the repeatability measurements. The low values of the coefficient of variation show that for a given torque the applied bolt load prediction is repeatable. The highest variation occurred with the torque of 20 foot-pounds with approximately 2.5 percent variation. The highest torque values of 50 ft-lbs. varied by a little more than 1.1 percent. The consistency of the applied torque to the induced bolt load, is illustrated in Figure 4.2. A final equation was developed using the averages from each of the trials that gives the relationship between the applied torque and the resulting bolt load. The average bolt load vs. torque equation is shown with the resulting plot in Figure 4.3 where Y is the predicted bolt load in pounds and X is the applied torque in foot-pounds.

Table 4.1 – Bolt Load Trial Output (lbs)

Applied Torque (ft-lbs)	Trials						
	1	2	3	4	5	6	7
20	3344.4	3180.8	3059.8	3216.4	3251.9	3166.5	3195.0
25	4113.0	4013.3	3892.4	3984.9	4120.1	3977.8	3999.1
30	4881.5	4888.6	4717.8	4824.5	4881.5	4717.8	4803.2
35	5585.9	5735.4	5557.5	5600.2	5678.4	5479.2	5614.4
40	6247.7	6511.0	6336.6	6382.9	6425.6	6276.2	6304.6
45	6987.7	7279.5	7144.3	7122.9	7151.4	6973.5	7073.1
50	7628.2	7927.0	7749.1	7784.7	7777.6	7706.4	7827.4

Table 4.2 - Repeatability Statistics

Applied Torque (ft-lbs)	Mean	Standard Deviation	Coefficient of Variation
20	3202.1	80.146	0.025029084
25	4014.3	73.894	0.018407477
30	4816.4	69.035	0.014333412
35	5607.3	76.451	0.013634225
40	6354.9	85.102	0.013391472
45	7104.7	97.483	0.013720958
50	7771.5	86.854	0.011175937

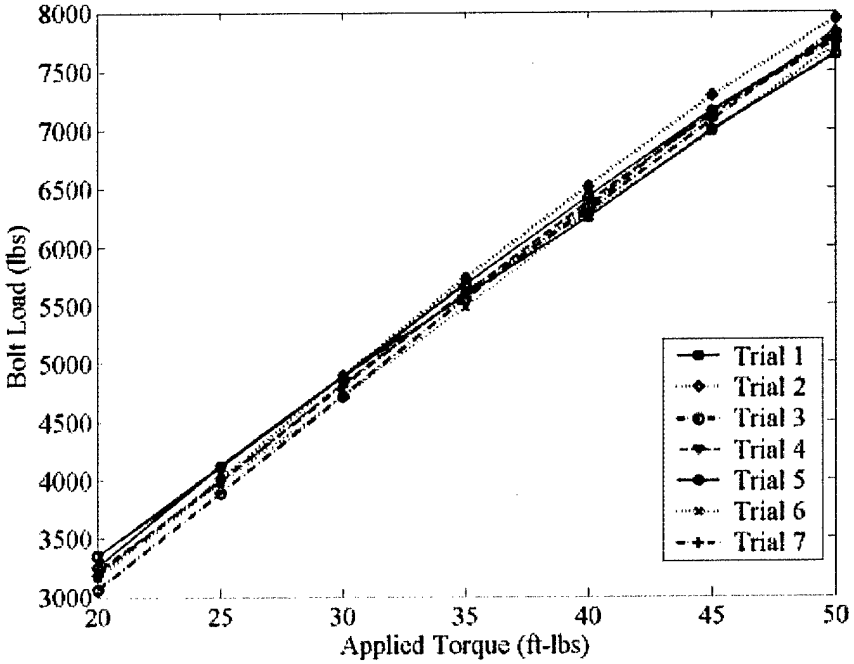

Figure 4.2 - Bolt Load vs. Torque for Seven Trials

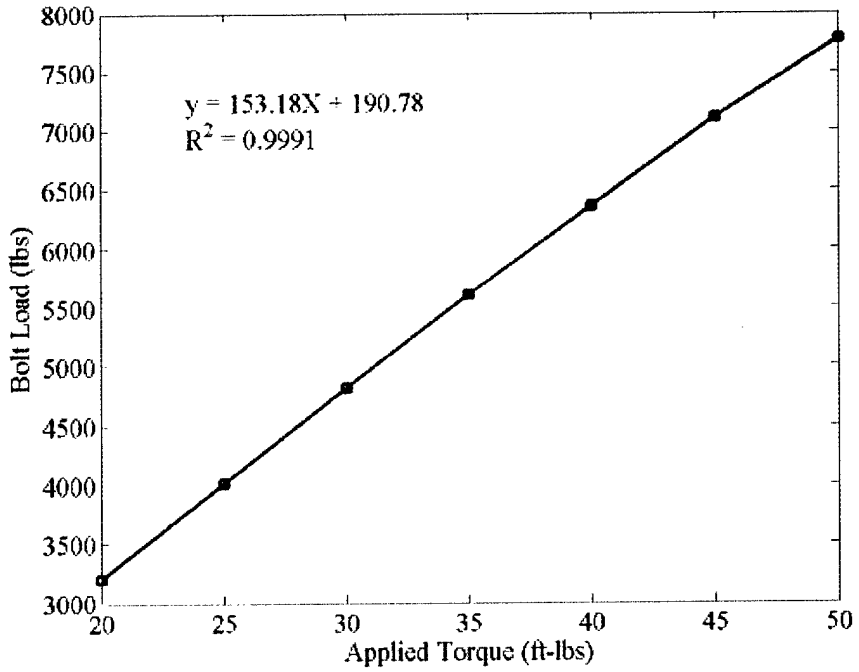

Figure 4.3 - Average Bolt Load versus Applied Torque

4.2 Change in Fundamental Frequency with Bolt Loosening

The effect of changing the bolt torque on the fundamental frequency of the structure is presented in this section. In this study the load on every bolt encompassing the perimeter of the plate was changed. Table 4.3 reports the natural frequency and the corresponding bolt load for each step in applied bolt torque. The results show that a change in the tension of the bolts around the perimeter of the plate does not significantly change the fundamental frequency of the plate. Figure 4.4 illustrates that the fundamental frequency does not show a dependency on the uniform clamping force around the plate perimeter. The only case that is remotely detectable is when all of the bolts are completely loose (0 applied torque).

Table 4.3 - Uniform Clamping Force Test Results

Applied Torque (in-lbs)	1st Nat Freq (Hz)	Bolt Voltage (mV)	Bolt Tension (lbs)
0	30.25	0.00	0.00
50	135.94	0.80	336.26
60	137.25	1.00	421.72
70	137.31	1.10	464.45
80	137.56	1.30	549.92
90	137.88	1.50	635.38
100	138.13	1.70	720.85
110	138.25	1.90	806.31
120	138.50	2.20	934.51
130	138.50	2.50	1062.70
140	138.81	2.70	1148.17
150	138.81	3.00	1276.36
160	139.06	3.20	1361.83
170	139.06	3.50	1490.02
200	139.38	4.20	1789.15
230	139.38	5.20	2216.47
300	139.63	7.40	3156.57
360	139.75	8.90	3797.55
480	139.81	11.60	4951.31
600	139.81	14.80	6318.74

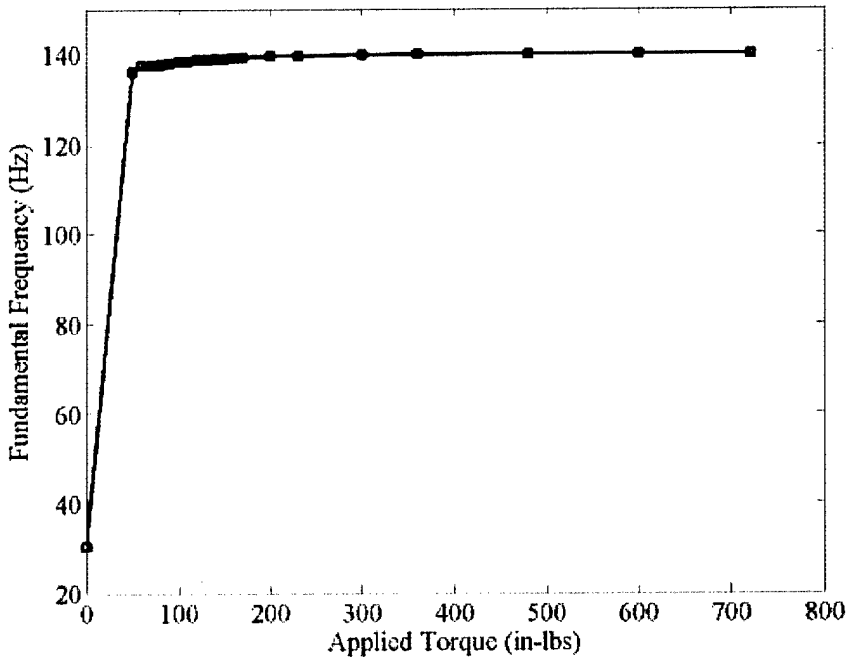

Figure 4.4 - Fundamental Frequency Dependency on Uniform Perimeter Torque

4.3 Change in Fundamental Frequency and Damping with Single Bolt Loosening

The effect of changing the bolt torque on the fundamental frequency of the structure, as a single bolt is loosened, is presented in this section. In this study, the load on only the instrumented bolt was changed as the other bolts were left at the full torque of 720 in-lbs. Figure 4.5 shows the measured natural frequency for each torque setting of the instrumented bolt only. There is almost no change in the fundamental frequency due to the effects of one bolt being loosened with the slope of the line being close to zero after the initial torque is applied. As expected, the results are less sensitive than those presented in Section 4.2, where there was no significant effect of the bolt torque on the fundamental frequency.

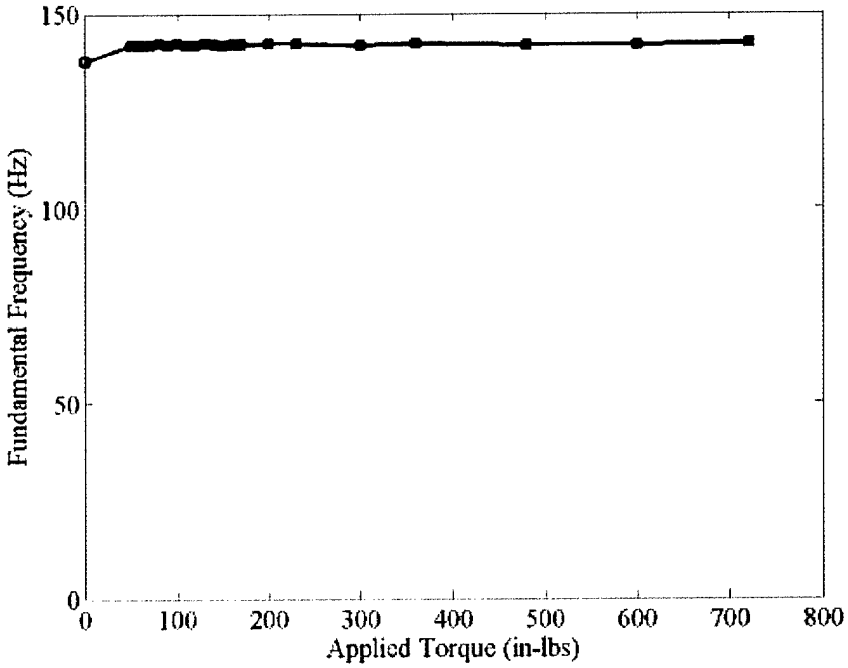

Figure 4.5 - Fundamental Frequency Dependency with Single Bolt Loosening

The effect of bolt torque on the damping coefficient for the fundamental frequency was also investigated. The damping coefficients were computed using the half-power bandwidth method. In this method, there are two points corresponding to half power points (3-dB smaller than the peak response). The damping coefficient is computed using

Equation (4.1), where ω_a and ω_b are the half-power frequencies and ω_d is the frequency corresponding to the maximum response.

$$\varsigma = \frac{\omega_b - \omega_a}{2\omega_d}, \tag{4.1}$$

Figure 4.6 is a representative plot of the transfer function, in the dB scale, about the fundamental frequency recorded during these tests. Figure 4.7 depicts the transfer function in a narrow region about the fundamental frequency and the half-power frequencies used in calculating the damping coefficient. The Matlab program written to compute the damping coefficient from the transfer function data is available in Appendix F. Figure 4.8 is a plot of the damping coefficients as a function of applied bolt torque on the single bolt that was loosened. The figure shows that there is no significant change in the level of damping when the torque on one of the sixteen bolts is altered.

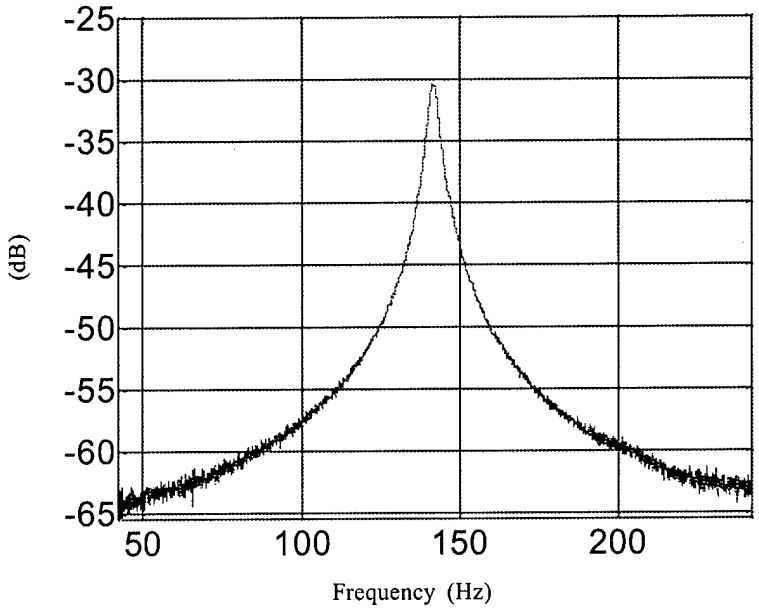

Figure 4.6 - Frequency Response about the Fundamental Frequency

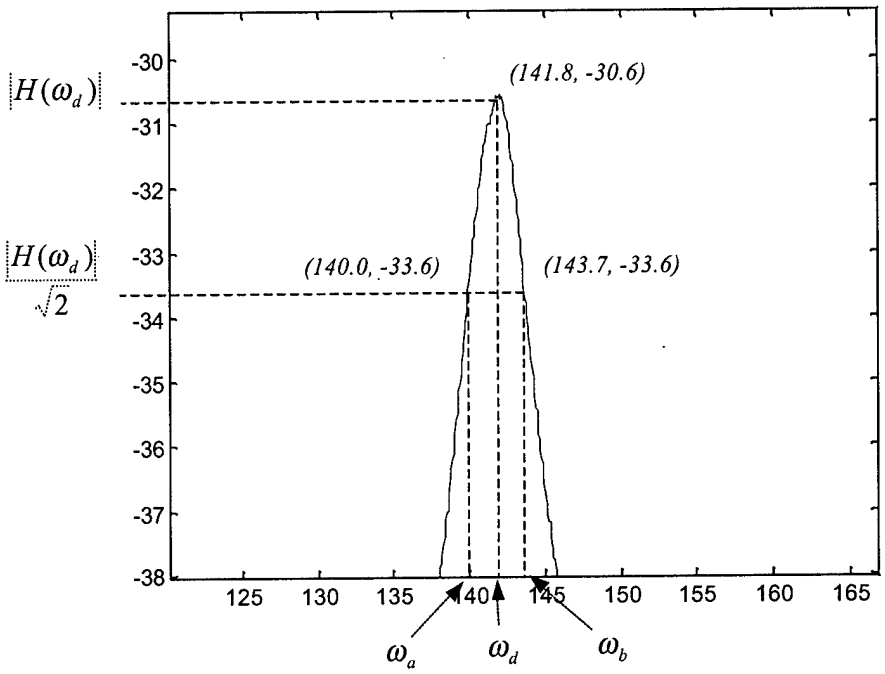

Figure 4.7 - Damping Estimation Illustration

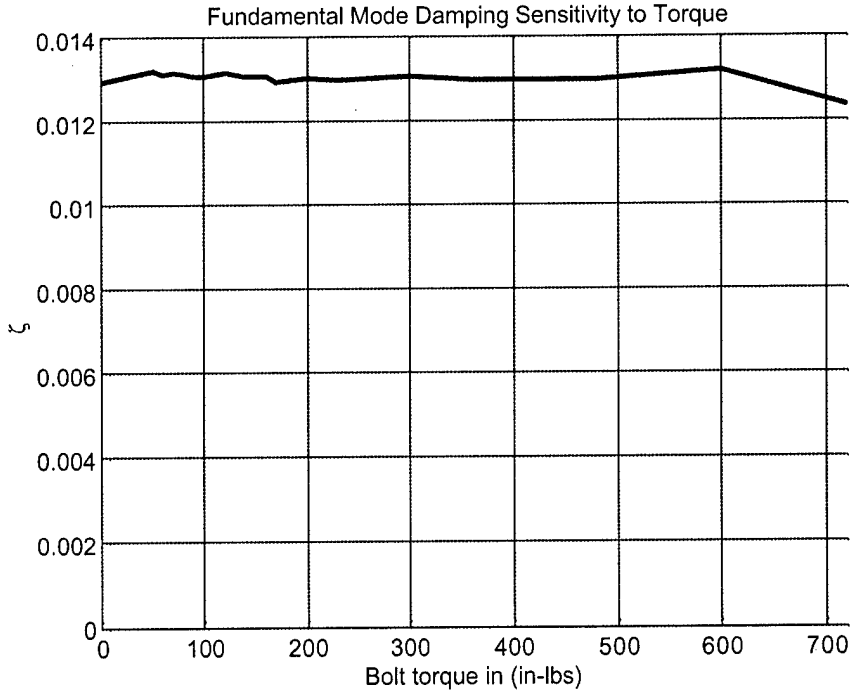

Figure 4.8 - Fundamental Mode Damping Sensitivity to Torque

4.4 Use of Transfer Functions at High Frequency to Detect Loosening

The high frequency tests were conducted using both the dynamic strain sensors and the shear accelerometers, along with transfer function information, to detect bolt loosening of a single bolt. Tests 1 and 2 were conducted with the dynamic strain sensors, while test number 3 was conducted with the shear accelerometers. The two tests using the dynamic sensors were conducted to observe the differences in the results between tests performed on different days. Figures 4.9, 4.10 and 4.11 show the recorded transfer functions of tests 1, 2 and 3 respectively for the sensors next to the loosened bolt. Figures 4.12, 4.13 and 4.14 show the recorded transfer functions for tests 1, 2, and 3 respectively for the sensors away from the loosened bolt. The plots show the response measured on the decibel scale as a function of both the loosened bolt load and frequency range investigated. The figures show that the transfer functions change as the bolt load is reduced. The change of the transfer functions as the load is changed is quantified with the damage index (D):

$$D = \frac{\int_{f_1}^{f_2} |T_h - T_d| df}{\int_{f_1}^{f_2} |T_h| df} \tag{4.2}$$

The frequency range used to calculate the damage index is denoted by f_1 and f_2. T_h is the reference healthy transfer function when all of the bolts are torqued to the same value. T_d represents the transfer functions for the damaged system, which in this case is due to a loose bolt. Plots of the damage index for tests 1, 2 and 3 are shown in Figures 4.15, 4.16 and 4.17, respectively. Inspection of the damage index plots show an increasing change in the damage index integral ratio as the bolt is loosened.

The damage index plots do not show significant dependence on the location of the sensors relative to the loosened bolt. The transfer function plots change as the bolt load varies, and thus the damage index plots change. The results do show that there is a change in the dynamic characteristics of the system with a bolt loosening, and that the sensitivity to the changes are different depending on what type of sensor is used. The damage index plots for dynamic strain sensors shows that there are greater changes for the sensor away from the bolt, than the sensor next to the loosened bolt as seen in Figures

4.15 and 4.16. The damage index plot using the accelerometers (test 3) shows a larger damage index response for the sensor located closer to the loosened bolt, and a smaller damage index response for the sensor placed on the opposite side of the plate in Figure 4.17.

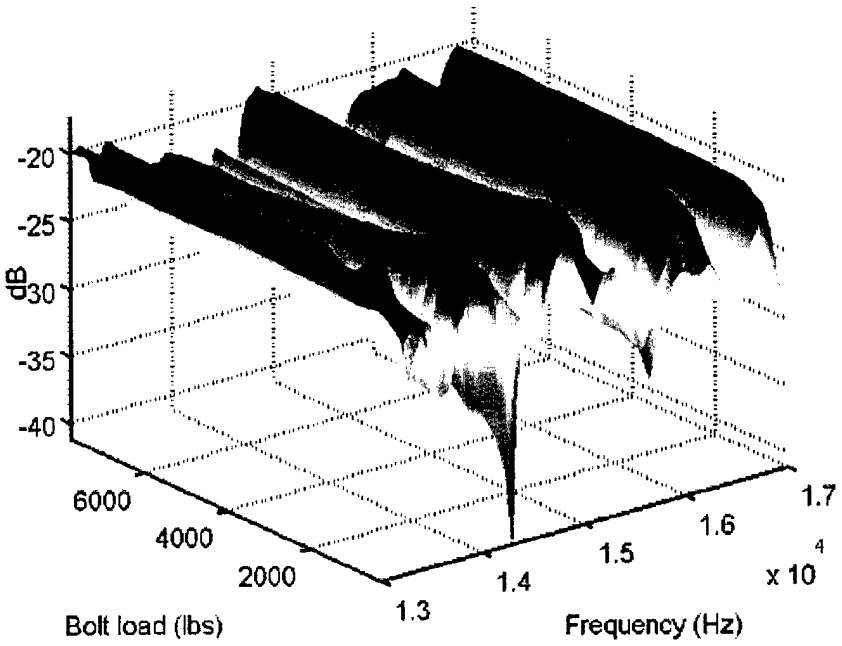

Figure 4.9 - Test 1 Transfer Functions for Sensor Next to the Bolt

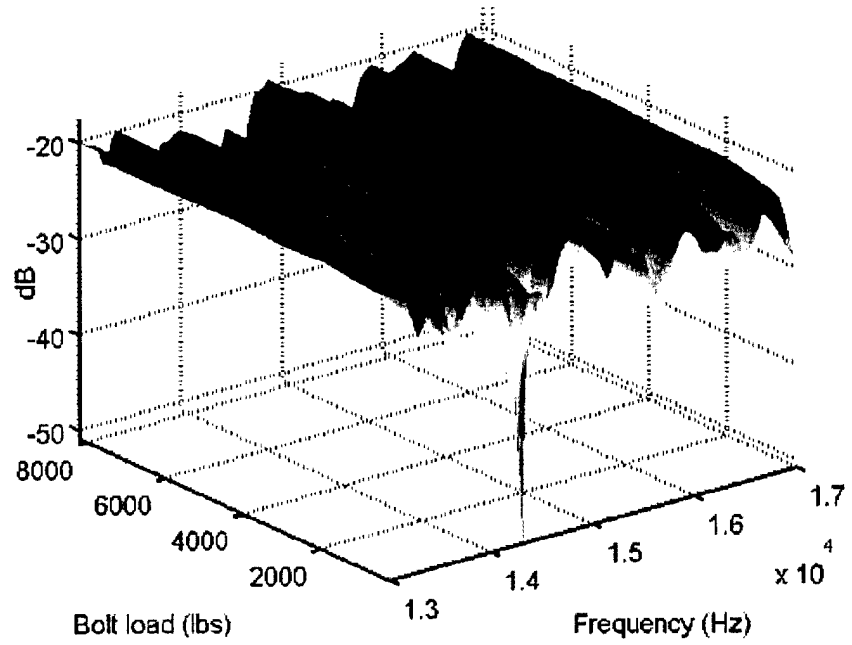

Figure 4.10 - Test 2 Transfer Functions for Sensor Next to the Bolt

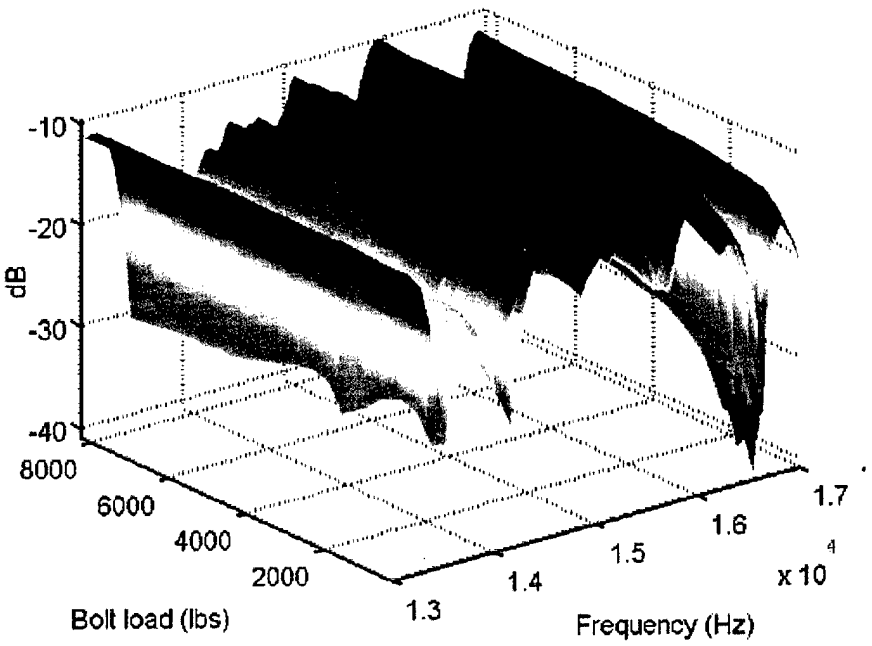

Figure 4.11 - Test 3 Transfer Functions for Sensor Next to the Bolt

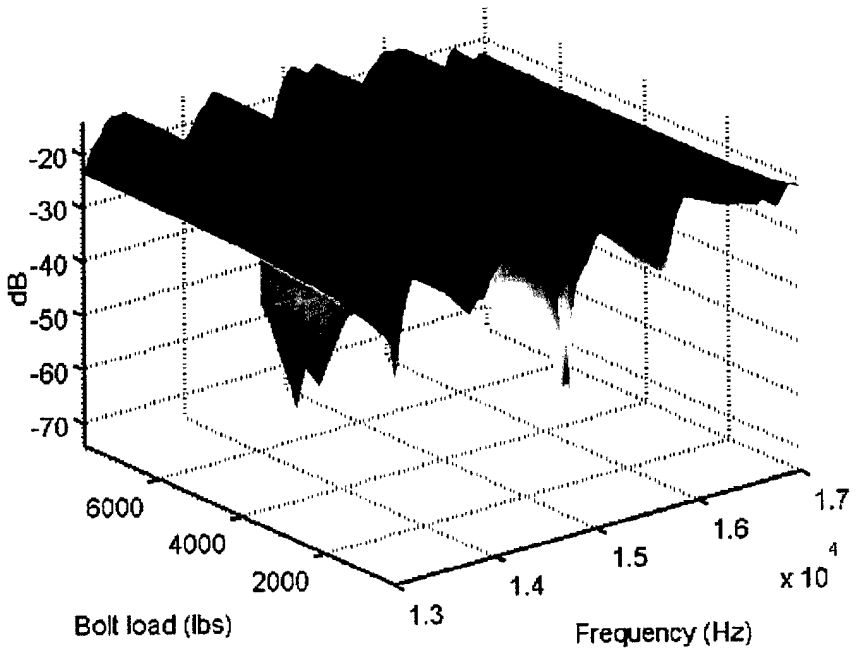

Figure 4.12 - Test 1 Transfer Functions for Sensor Away from the Bolt

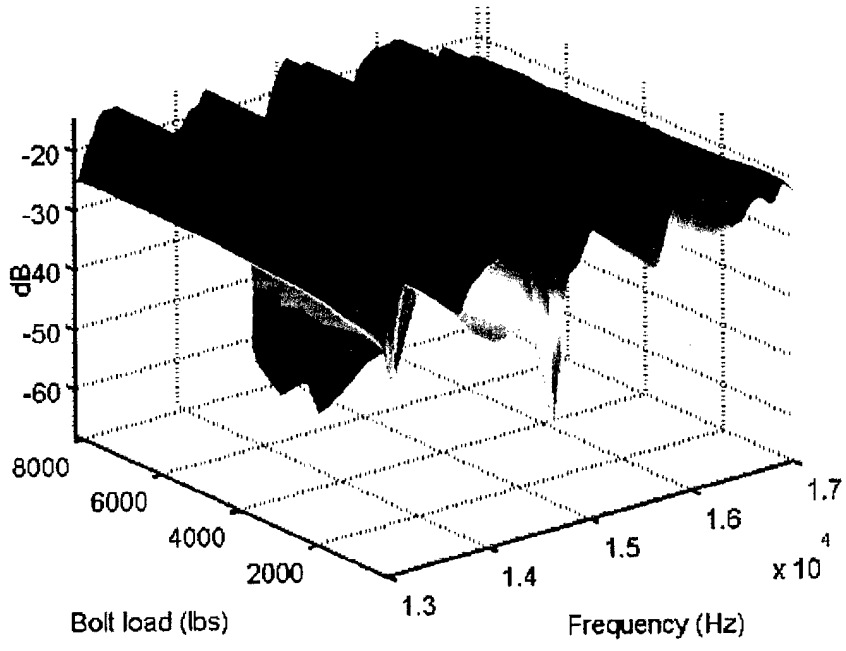

Figure 4.13 - Test 2 Transfer Functions for Sensor Away from the Bolt

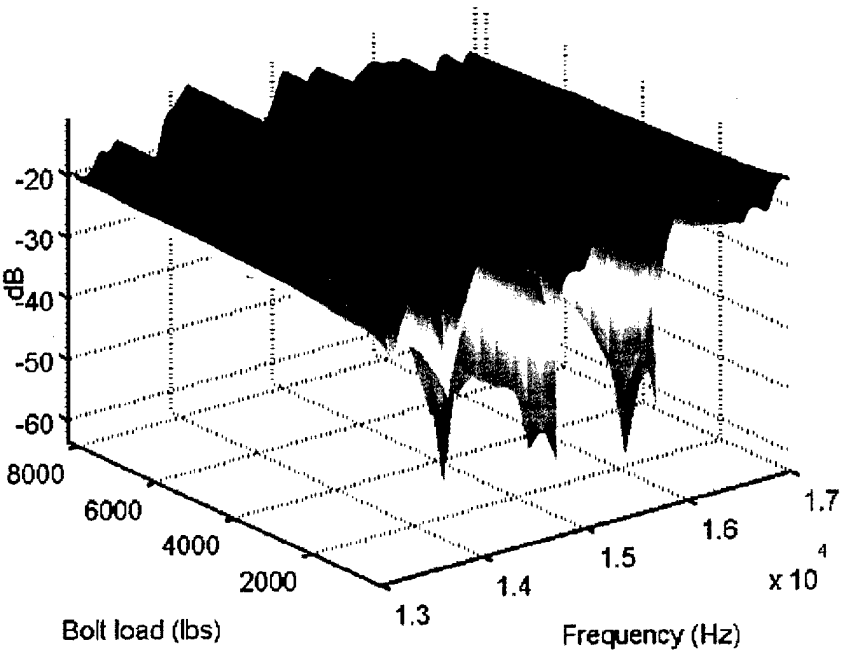

Figure 4.14 - Test 3 Transfer Functions for Sensor Away From the Bolt

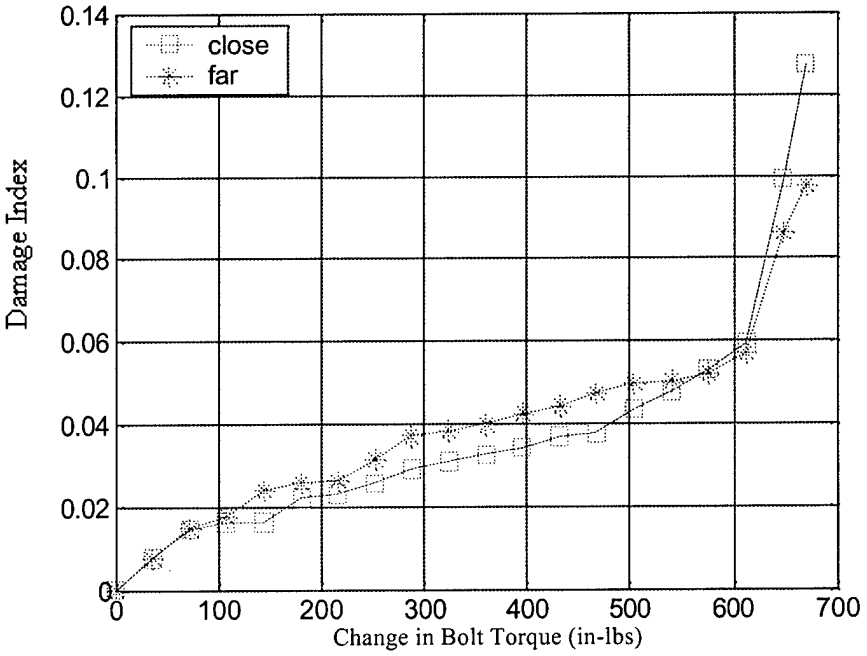

Figure 4.15 - Loosening Indicator for Test 1

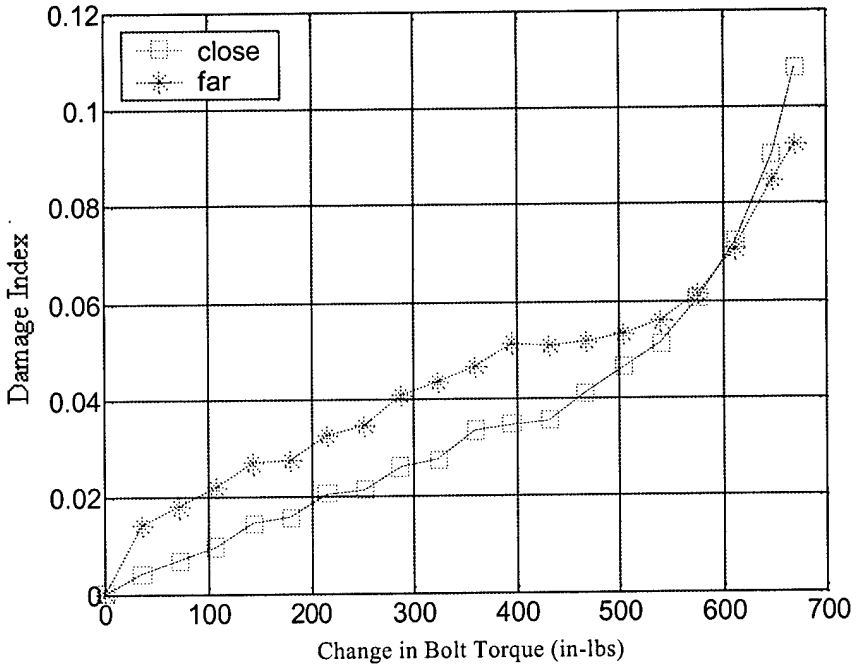

Figure 4.16 - Loosening Indicator for Test 2

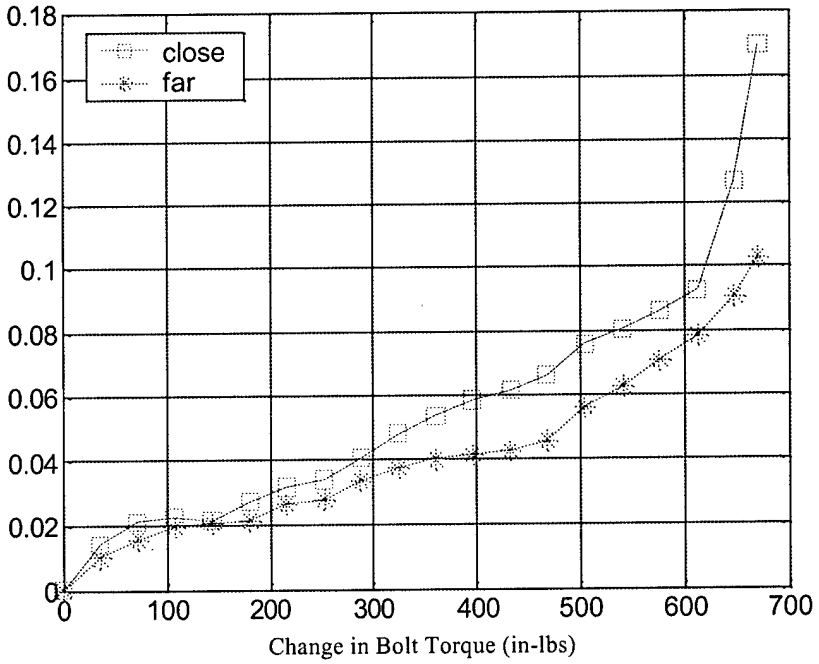

Figure 4.17 - Loosening Indicator for Test 3

The results presented in this section show that change in the boundary conditions of a bolted plate could be detected using the high frequency transfer functions technique. However, the dynamic strain sensors were not able to accurately predict the location of the loosened bolt. A higher damage index is obtained for the sensor far away from the damage than a sensor located closer to the loosened bolt. The accelerometer test returned a larger damage index for the sensor next to the loosened bolt, but the difference between the indices values were not significantly large. In the transfer function experiments, the experimenter had the benefit of knowing the damage location, and placed a sensor near that location. However, this is not possible in practical applications.

4.5 Detection of Bolt Loosening Using Transmittance Functions

Transmittance function estimates were made in the frequency range from 0 Hz to 20 kHz. Various sub-ranges were investigated to determine the best range in which to detect bolt loosening. The frequency investigation was done by splicing together five smaller successive 3 kHz bandwidth test results. Smaller bandwidths allowed a higher frequency resolution than would be possible if the sample were taken over the entire 0-20 kHz range. Damage indices were calculated, as per equation 4.2, for different bandwidths within the entire range, and the bandwidths were chosen to maximize the damage index where the damage occurred. Larger damage indices were found using the accelerometers over the dynamic strain sensors. Two different frequency ranges, or bandwidths, were found to produce the greatest damage indices for T23 and T32 when the instrumented bolt was loosened. The results from the accelerometer plots are shown in Figures 4.18 and 4.19. Figure 4.18 corresponds to the lower frequency bandwidth of 7 kHz to 9 kHz, and Figure 4.19 is for the 18 kHz to 20 kHz bandwidth. Both figures show the computed damage indices values, the transmittance function plots for each torque setting as a function of the frequency, and the difference (delta) between each torque setting and the "healthy" setting of 720 in- lbs .

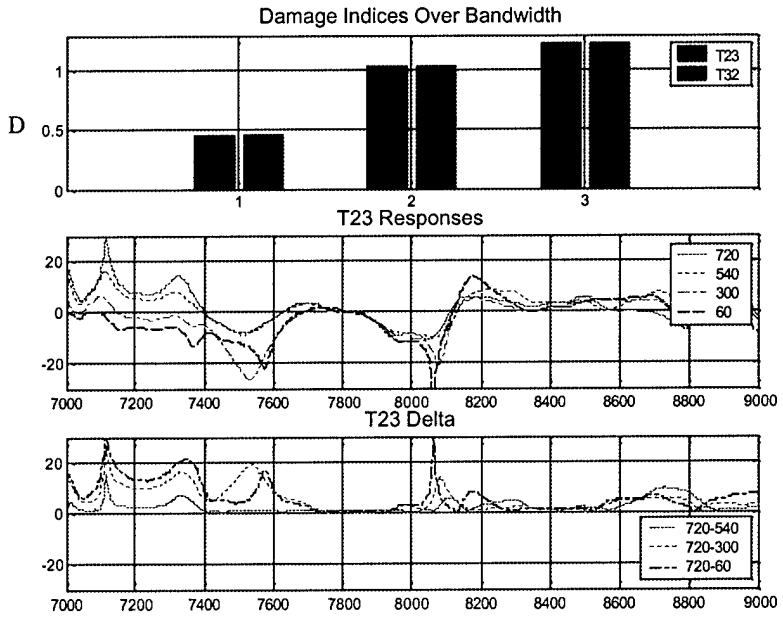

Figure 4.18 - Investigation Using Accelerometers at 7 kHz to 9 kHz.

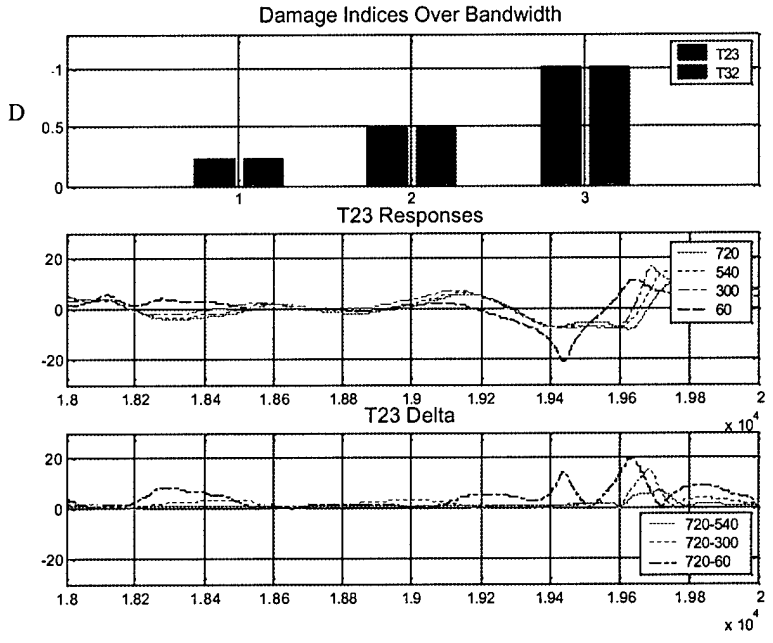

Figure 4.19 - Investigation Using Accelerometers at 18 kHz to 20 kHz.

The calculated damage indices were larger for the 7 kHz to 9 kHz range than the damage indices calculated in the 18 kHz to 20 kHz range. The results for the dynamic strain sensor tests are shown in Figures 4.20 and 4.21. The dynamic strain sensors were not as sensitive to the level of damage in the plate as were the accelerometers, as indicated by the smaller magnitude of the damage indices. However, the dynamic strain sensors were able to show the successive levels of bolt loosening in the system.

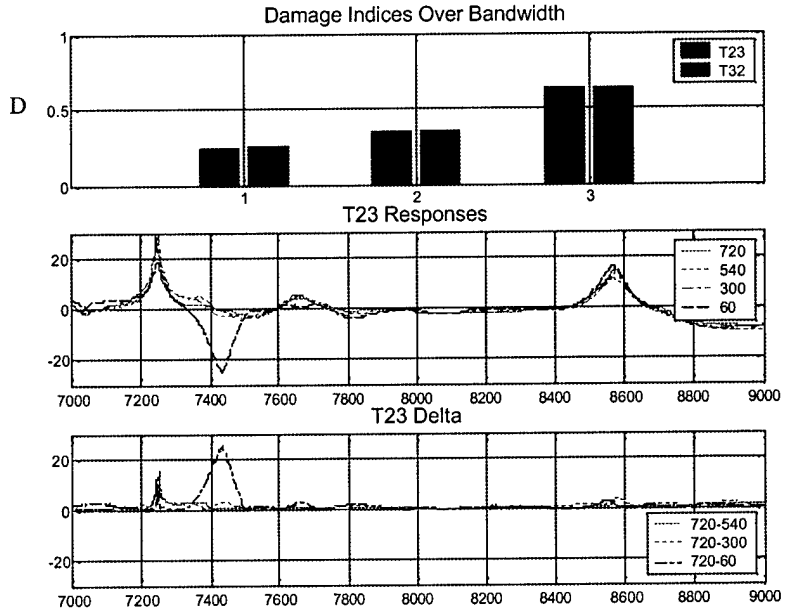

Figure 4.20 - 7 kHz to 9 kHz Investigation Using Dynamic Strain Sensors

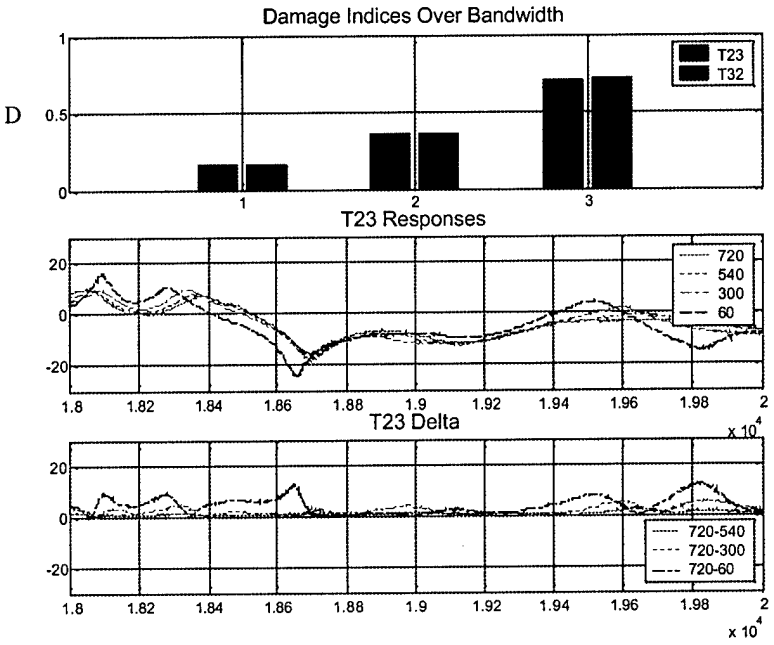

Figure 4.21 – 18 kHz to 20 kHz Investigation Using Dynamic Strain Sensors

4.5.1 Transmittance Functions to Detect Reduction of Torque on One Bolt

Detection of bolt loosening of a single bolt using transmittance functions was demonstrated by placing a sensor at each of the four corners of the bolted composite plate as described previously in Section 3.3. Extensive transmittance testing using accelerometers over the frequency ranges determined in Section 4.5 showed that a bolt loosened between sensors 2 and 3 could be detected as depicted in Figure 4.22. The damage levels for the transmittance function T23 was higher than all other reported transmittance functions in the 7 kHz to 9 kHz frequency range when using accelerometers as sensors. Thus, according to Figure 4.22 the transmittance testing technique indicated that there were significant changes between sensors 2 and 3, which was the location of the bolt that was loosened.

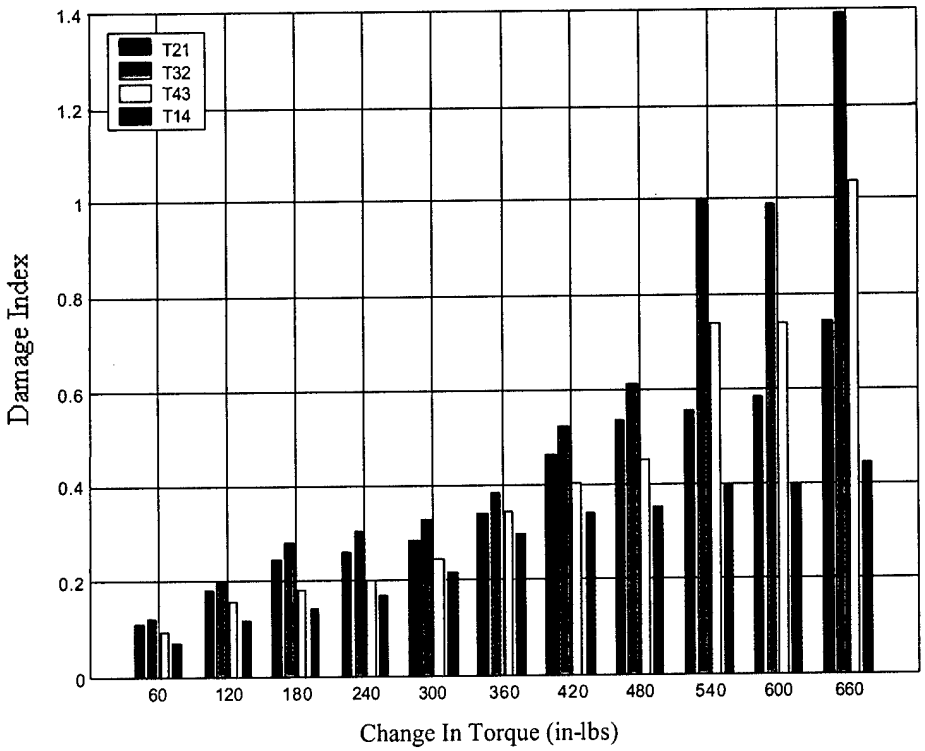

Figure 4.22 - Damage Indices for 7 kHz to 9 kHz Freq. Range Using Accelerometers

Figure 4.23 depicts the damage indices for the transmittance functions measured using accelerometers for the frequency range of 18 kHz to 20 kHz. The results, as shown in Figure 4.23, do not show as strong of a sensitivity to the bolt loosening as the transmittance results for the 7 kHz to 9 kHz range shown in Figure 4.22. Even so, a strong trend still does exist. The T23 damage index values were not always the largest damage index as shown for the 7 kHz to 9 kHz in Figure 4.22. The lower and intermediate changes in bolt torque tests, such as the 420 in-lbs. torque change in Figure 4.23, show a larger damage index for T12 than T23. It is expected that T12 would show considerable sensitivity to the loosened bolt in these experiments, because Sensor 2 is close to the bolt being loosened. Thus it is reasonable that the bolt being loosened in its proximity affected sensor 2's response. However, for the two frequency ranges investigated using accelerometers the 7 kHz to 9 kHz range produced better results. Tests conducted using both frequency ranges

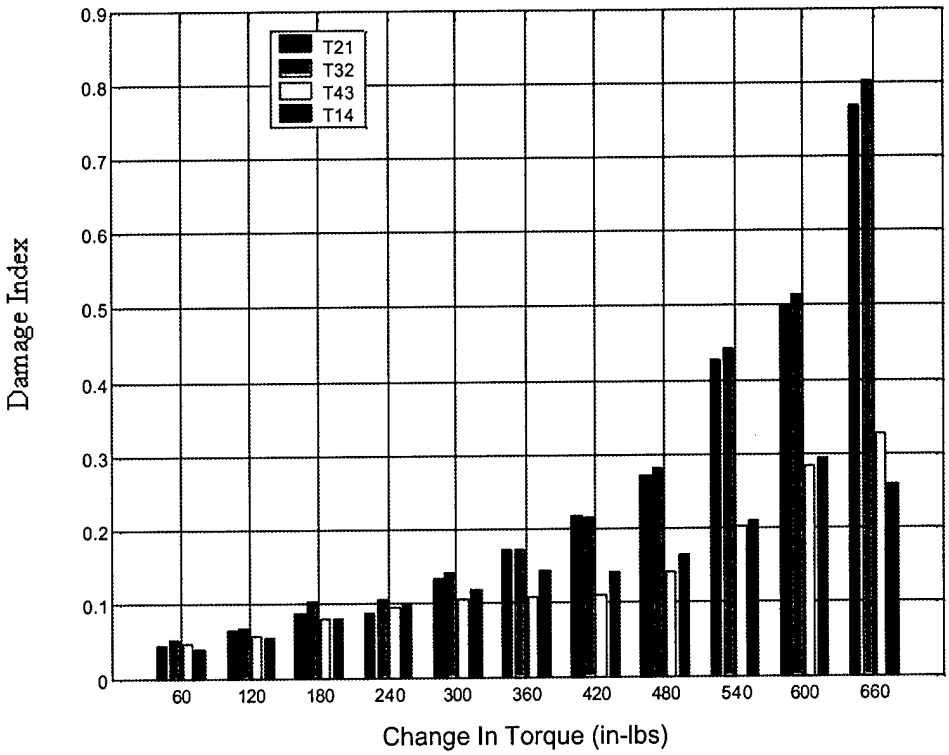

Figure 4.23 - Damage Indices for 18 kHz to 20 kHz Using Accelerometers

showed increasing damage indices for all transmittance functions as the bolt was progressively loosened.

The transmittance tests were repeated using the dynamic strain sensors. The higher frequency range of 18 kHz to 20 kHz gave the T23 damage index as the maximum index only when there was a large change in the bolt torque, such as 480 in-lbs and higher. T43 showed the largest damage index values for the lower change in torque tests, and had the second largest damage index for the high change in torque tests. These results are reported in Figure 4.24. The transmittance test results for the dynamic strain sensor in the 7 kHz to 9 kHz range did not show any correlation between the damage indices and actual damage locations.

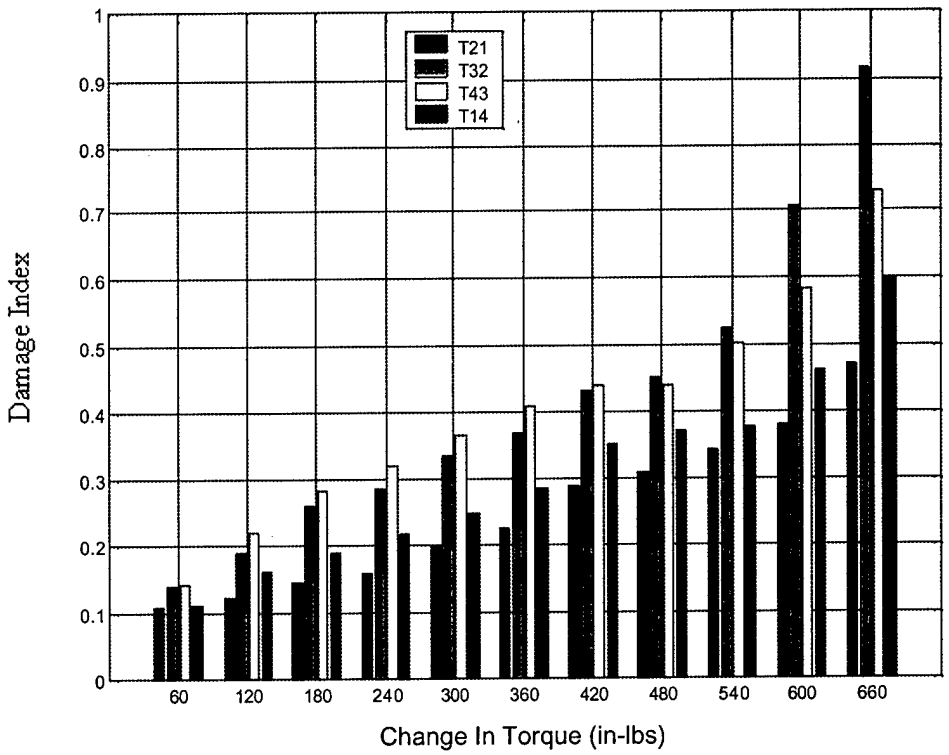

Figure 4.24 - Damage Indices for 18 kHz to 20 kHz Using Dynamic Strain Sensors

4.5.2 Repeatability of Transmittance Function Data

The repeatability of the most promising transmittance results was investigated. The damage index for T23 and T32 were calculated using accelerometers for the 7 kHz to 9 kHz frequency range. The tests showed damage indices calculated from the transmittance functions had some variation. The T23 damage indices had a minimum of 0.677 and a maximum of 0.758, or +/-0.041, which is approximately 6% of the smaller value. The largest variation was in the transmittance pair T23 and T32 as shown in Figure 4.25. The other damage indices results exhibited less variation than T23.

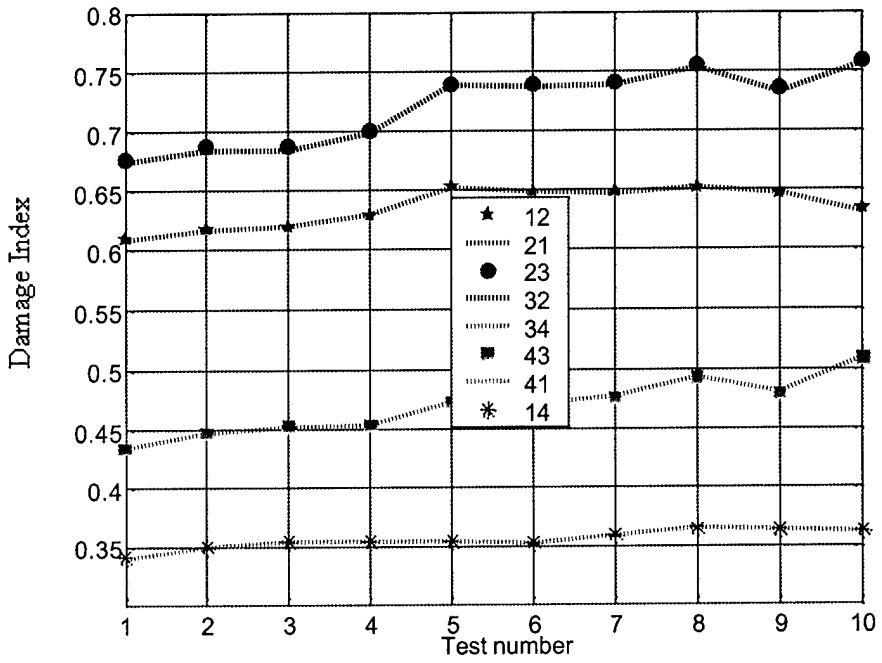

Figure 4.25 - Transmittance Function Repeatability

4.5.3 Bolt Loosened at a Different Location

The previous work for locating the damage source on a plate used the same loosened bolt location. The frequency range investigation was conducted to maximize the damage detection that occurred between sensors 2 and 3. The next set of experiments was performed by loosening a bolt between sensors 1 and 4. Figure 4.26 plots the damage indices levels found from the transmittance functions. The results displayed show that the method investigated thus far is sensitive to relaxation of the bolt force, but is not reliable in successfully locating the loosened bolt. If the location detection method worked as hypothesized, then T14 should have been greater than the other transmittance pairs for each torque setting. As Figure 4.26 shows, the damage index for T14 is not the largest for each change in bolt torque, and T14 even has the smallest damage index for the largest change in bolt torque. However, since the average damage index is large, the method is still capable of detecting whether or not the load in one or more bolts, on a panel, has relaxed. The method can not, as of yet, be used to determine the location of the loosened bolt.

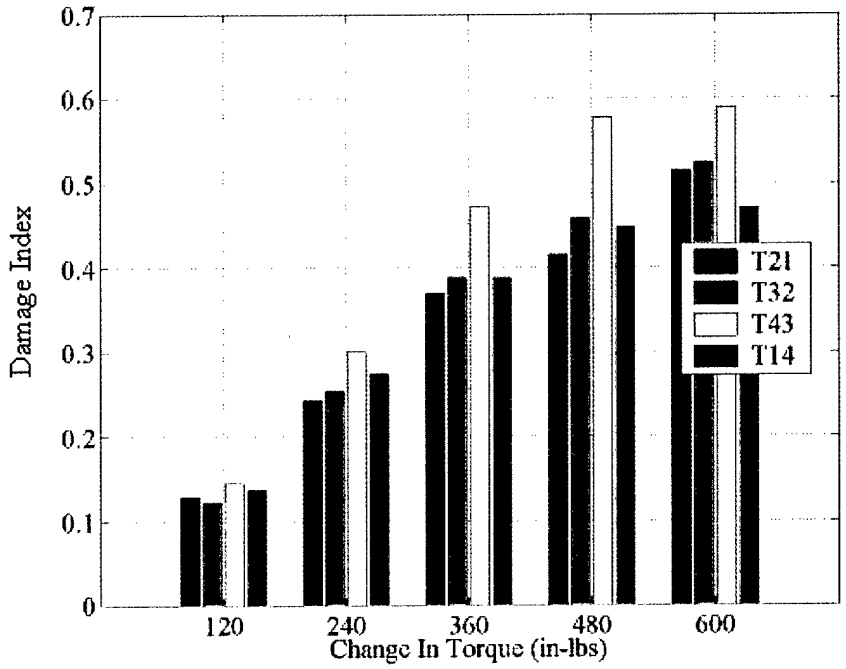

Figure 4.26 -Damage Indices for Bolt Loosened at a Different Location

5. SUMMARY AND CONCLUSIONS

Various vibration-based methods for detection of bolt loosening in hybrid composite/metal bolted connections have been investigated. The methods performed in this study include: 1) Changes in fundamental frequency; 2) Changes in damage index measured using high frequency transfer functions; and 3) Changes in damage index measured using high frequency transmittance functions. A proof-of-concept test bed for this study consisted of a 24-½ inch square EGlass/Vinyl ester composite panel bolted to a steel framework. The composite was bolted to the steel at its perimeter using 16 – ½-inch diameter bolts, with one of the bolts being instrumented. A series of tests were performed on this panel to assess the potential for implementation of various methods in detecting loosening of one or more bolts.

The study began by looking into the feasibility of detecting bolt loosening through changes in the structure's fundamental frequency. These test results show that the fundamental frequency is insensitive to changes in the bolt torque as one or more bolts are loosened. The only case that could readily be detected by this method is the one where all 16 bolts are completely loose. Use of damping ratio at the fundamental frequency to detect loosening was also investigated and the same conclusion was drawn.

The changes of transfer functions from sensors located next to, and away from, a loosened bolt were also investigated for frequencies well outside the first several natural frequencies of the structure. The range from 0-20 KHz was investigated. The transfer function changes were quantified through a scalar damage index. It was found that excitation between 13 KHz and 17 KHz provided a damage index that was sensitive to bolt torque. However the transfer function technique used herein was not suited to locate the position of a single loosened bolt.

A thorough investigation of using transmittance techniques to assess bolt loosening was also presented. Two different frequency ranges were assessed (7-9 KHz and 18-20KHz) to determine in which range the transmittance function damage index was most sensitive to localized changes. The initial bolt loosening investigation showed that when using accelerometers capable of measuring the normal acceleration of the plate excited by

a chirp function, localized bolt loosening could be detected. The ideal frequency range to excite the plate with a chirp function was found to be 7 kHz to 9 kHz. These results were determined to be repeatable. However, the transmittance method also had difficulty in detecting the location of a loosened bolt. If a bolt was loosened on the opposite side of the plate, the transmittance method was not successful in determining the location.

Both the transfer function and the transmittance function methods presented herein are capable of detecting a change in the system. This change is detectable for small amounts of stress relaxation and even if only one bolt was loosened. The final conclusion is that the transfer and transmittance function methods were successful in detecting the change, but were not successful in pin pointing the location of the loosened bolt.

5.1 Recommendations

The transmittance function technique shows promise for assessment of bolt loosening in a two-dimensional structure, but its implementation needs further investigation. Future investigations should include the sensitivity at even higher frequencies of excitation. It is recommended that the details of the system be investigated on a simpler structure, such as a beam, and ultimately applied to plate and shell structures. Environmental conditions of the structure will play a key role in the structural performance and needs to be investigated. Implementation of the techniques with the structure under various conditions, such as hot and submerged, should be attempted to assess the robustness of the method.

This investigation was limited to 20 kHz because of hardware constraints, but similar Siglab units are capable of analysis up to 50 kHz. Also, the addition of more sensors to the detection scheme may produce better results, but would make the system more complex and expensive. A finite element simulation of both the transfer function and transmittance function methods, for rectangular beams and plates, would prove useful in deciding whether this method is advantageous, and would aid in optimal sensor and actuator placement.

REFERENCES

ABAQUS Users Manual, 2002, Version 6.3, Hibbit, Karlson & Sorensen, Inc.

Banks, H. T., Emeric, P. R., 1998, Detection of Non-Symmetrical Damage in Smart Plate-Like Structures, *Journal of Intelligent Material Systems and Structures*, Vol. 9, pp. 818-828.

Berman, J., Quattrone, R., Averbuch, A., Lalande, F., Cudney, H., Raju, V., Cohen, G.L., 1999, *Piezoelectric Patch Sensors for Structural Integrity Monitoring of Composite-Upgraded Masonry and Concrete Structures*, US Army Corps of Engineers, Construction Engineering Research Laboratory, CERL Technical Report 99/72.

Caccese, V., 2001, Modular Advanced Composite Hull-form (MACH) Technology, Proposal funded by Office of Naval Research Project Number 5-6-46601, University of Maine.

Doebling, S. W., Farrar, C. R., Prime, M. B., Shevitz, D. W., 1996, Damage Identification and Health Monitoring of Structural and Mechanical Systems From Changes in Their Vibration Characteristics: A Literature Survey, Los Alamos National Laboratory, Report No. LA-12767-MS, Los Alamos, NM.

Farrar, C.R., Doebling, S.W., 1997, An Overview of Modal-Based Damage Identification Methods, *Proceedings of DAMAS Conference*, Sheffield, UK.

Fugate, M. L., Sohn, H., Farrar, C. R., 2001, Vibration-Based Damage Detection Using Statistical Process Control, *Mechanical Systems and Signal Processing*, Vol. 15, No. 4, pp. 707-721.

Ganguli, R., 2001, A Fuzzy Logic System for Ground Based Structural Health Monitoring of a Helicopter Rotor Using Modal Data, *Journal of Intelligent Material Systems and Structures*, Vol. 12, pp. 397-407.

Ghoshal, A., Sundaresan, M. J., Schulz, M. J., Pai, P. F., 2000, Structural Health Monitoring Techniques for Wind Turbine Blades, *Journal of Wind Engineering and Industrial Aerodynamics*, Vol. 85, pp. 309-324.

Inman, D. J., 2001, *Engineering Vibrations*, Prentice Hall, New Jersey.

Kabeya, K., 1998, *Structural Health Monitoring Using Multiple Piezoelectric Sensors And Actuators*, Master's Thesis, Virginia Polytechnic Institute and State University.

Kessler, S. S., Spearing, S. M., Atalla, M J., Cesnik, C. E. S., Soutis, C., 2002, Damage Detection in Composite Materials Using Frequency Response Methods, *Composites: Part B*, Vol. 33, pp. 87-95.

Kim, J.-T., Stubbs, N., 2002, Improved Damage Identification Method Based on Modal Information, *Journal of Sound and Vibration*, Vol. 252, No. 2, pp. 223-238.

Kuo, E.Y, Jayasuriya, A.M.M., 2002, A High Mileage Vehicle Body Joint Degradation Estimation Method, *International Journal of Materials and Product Technology*, Vol. 17, Nos. 5/6, pp. 400-410.

Lew, J. S., Juang, J.N., 2002, Structural Damage Detection Using Virtual Passive Controllers, *Journal of Guidance, Control, and Dynamics*, Vol. 25, No. 3, pp. 419-424.

Park, G., Cudney, H. H., Inman, D. J., 2000, An Integrated Health Monitoring Technique Using Structural Impedance Sensors, *Journal of Intelligent Material Systems and Structures*, Vol. 11, pp. 448-455.

Park, K. C., Reich, G. W., Alvin, K.F., 1998, Structural Damage Detection Using Localized Flexibilities, *Journal of Intelligent Material Systems and Structures*, Vol. 9, pp. 911-919.

Robbins, D. H., Reddy, J. N., 1991, Analysis of Piezoelectrically Actuated Beams Using a Layer-Wise Displacement Theory, *Computers and Structures*, Vol. 41, pp. 265-279.

Salawu, O. S., 1997, Detection of Structural Damage Through Changes in Frequency: A Review, *Engineering Structures*, Vol. 19, No. 9, pp. 718-723.

Schulz, M.J., Abdelnaser, A.S., Pai, P.F., Linville, M.S., Chung, J., 1997, Detecting Structural Damage Using Transmittance Functions, *International Modal Analysis Conference*, Orlando, Florida.

Schulz, M.J., Pai, P.F., Inman, D.J., 1999, Health Monitoring and Active Control of Composite Structures Using Piezoceramic Patches, *Composites: Part B*, Vol. 30, pp. 713-725.

Tiersten, H. F., 1969, *Linear piezoelectric plate vibrations*, Plenum Press, New York.

Todd, M. D., Nichols, J. M., Pecora, L. M., Virgin, L. N., 2001, Vibration-Based Damage Assessment Utilizing State Space Geometry Changes: Local Attractor Variance Ratio, *Smart Materials and Structures*, Vol. 10, pp. 1000-1008.

Vel, S. S., Batra, R C., 2001, Exact Solution for Rectangular Sandwich Plates With Embedded Piezoelectric Shear Actuators, *AIAA Journal*, Vol. 39, pp. 1363-1373.

Vel, S. S., Batra, R. C, 2000, Cylindrical Bending of Laminated Plates with Distributed and Segmented Piezoelectric Actuators/Sensors, *AIAA Journal*, Vol. 38, pp. 857-867.

Vel, S. S., Batra, R. C., 2000, Three-Dimensional Analytical Solution for Hybrid Multilayered Piezoelectric Plates. *Journal of Applied Mechanics*, Vol. 67, pp. 558-567.

Vel, S. S., Batra, R. C., 2001, Exact Solution for the Cylindrical Bending of Laminated Plates With Embedded Shear Actuators, *Smart Materials and Structures*, Vol. 10, pp. 240-251.

Wang, D. H., Huang, S. L., 2000, Health Monitoring and Diagnosis for Flexible Structures with PVDF Piezoelectric Film Sensor Array, *Journal of Intelligent Material Systems and Structures*, Vol. 11, pp. 482-491.

Yan, Y. J., Yam, L. H., 2002, Online Detection of Crack Damage in Composite Plates Using Embedded Piezoelectric Actuators/Sensors and Wavelet Analysis, *Composite Structures*, Vol. 58, pp. 29-38.

Zak, A., Krawczuk, M., Ostachowicz, W., 2000, Numerical and Experimental Investigation of Free Vibration of Multiplayer Delaminated Composite Beams and Plates, *Computational Mechanics*, Vol. 26, pp. 309-315.

Zhang, H., Schulz, M. J,, Ferguson, F., 1999, Structural Health Monitoring Using Transmittance Functions, *Mechanical Systems and Signal Processing*, Vol. 13, No. 5, pp. 765-787.

Zou, Y., Tong, L., Steven, G. P., 2000, Vibration-Based Model-Dependent Damage (Delamination) Identification and Health Monitoring for Composite Structures—A Review, *Journal of Sound and Vibration*, Vol. 230, No. 2, pp. 357-378.

Zubaydi, A., Haddara, M.R., Swamidas, A.S.J., 2002, Damage Identification in a Ship's Structure Using Neural Networks, *Ocean Engineering*, Vol. 29, pp. 1187-1200.

APPENDIX A

Instrumented Bolt Information and Calibration

A.L. DESIGN, INC. 1411 Military Road, Buffalo, NY 14217, USA (716) 875-6240
FAX (716) 875-2404

A FEW PRACTICAL SUGGESTIONS ON THE BEST WAY TO USE LOAD CELLS, LOAD WASHERS AND FORCE TRANSDUCERS

Load Cells are generally used to measure and detect forces or changes in the magnitude of forces.

The ideal way to set up load cells is to mount them on a rigid (very rigid) base. This base could be a thick flat steel plate which should be hardened to Rockwell 44C or higher and ground flat with a surface grinder. The top plate should be just as strong as the bottom one.

Don't use soft steel plates or copper, aluminum or plastic plates. The soft materials will cause large errors. (High hysteresis, nonlinearity and non-repeatability.)

Whenever possible use load buttons with spherical surfaces. These will concentrate the applied force on the center of the load cell. If there is no room for load buttons on top and bottom try to use at least one at the top. If there is no room for load buttons then it is important to make sure that the two surfaces which come in contact with the load cell are parallel. If they are not the load will be placed off center, resulting in less accurate results.

The practical usable range of a load cell is generally 10% to 100% capacity. If you exceed the capacity then obviously the unit is overloaded and permanent deformation may result (zero shift) or the unit could be crushed. Dropping calibrating weights on the cell even from a small height could crush the load cell. So be careful and slowly place the load on the load cell. Make sure the load cell is not slanted at an angle since it is important that it is positioned perfectly vertical or in line with the applied force (within +/- 0.5 degree or better). Make sure there are no side loads applied to the load cell unless it is specially designed to withstand side loading.

If the force or weight is below 10% of the load cell capacity then the errors will make the measurement less accurate, for example a 10,000 lb. capacity load cell with an accuracy of 0.2% FS (full scale) will give a 100 lb. weight +/- 20 lb. accuracy (The 0.2% of 10,000 is 20 lbs.) This is usually unacceptable. To get accurate results the force to be measured should be near the full capacity of the load cell. Of course other requirements may make this impractical.

When the load cell is hooked up to the readout/power supply the numbers may drift some due to the warmup requirement of the instrument and load cell. Even though the load cell is usually temperature compensated some zero drift is to be expected as the temperature changes. Readings and tests should be done after the whole unit is at uniform temperature and the zero balance adjusted. Creep in twenty minutes is to be expected in the range of 0.2 - 0.3% FS.

For accurate tests, calibration runs, etc., make several test runs. A minimum of three to five test runs would be adequate most of the time. A minimum of three calibration points should be selected (20%, 60%, 100% FS.). Of course the more points you have selected the more information you'll have about the performance of the unit. MAKE SURE THE LOAD IS NEVER LESS THAN 10% CAPACITY. (DON'T REDUCE THE LOAD TO ZERO DURING CALIBRATION RUNS.) You can get a zero reading after the tests are finished. Usually ten test runs are sufficient to get very reliable and accurate results.

Load washers are small load cells and it is important that load buttons are used on top and bottom for best performance. If no buttons are used the accuracy of the results will suffer.

If you use Load Washers to measure bolt tension make sure you use hardened washers between the underside of the bolt head and the Load Washer. These washers should be as thick as possible. These tests require quite elaborate set ups so consult us before making the tests.

When using the readout instruments/power supplies make sure that they are hooked up properly. The red and black wires should be connected to 10 or 5 Vdc power, the green and white wires to the signal indicator. After waiting for a few minutes (15 to 30) to allow the instrument and the transducer to warm up, the zero should be adjusted and the reading recorded. Now you can start the test runs and do your measurements. These recommendations are very general. If you have any specific questions call us and we will be glad to help you. (716-875-6240).

Sincerely,

Andrew Lenkei, P.E.

A.L.DESIGN, INC.
1411 MILITARY ROAD
BUFFALO, NEW YORK, 14217
U.S.A.

(716) 875-6240
FAX: (716)875-2404

THIS PROGRAM BY A.L.DESIGN, INC. CALCULATES THE NON LINEARITY, HYSTERESIS, REPEATABILITY, AND BEST FIT STRAIGHT LINE THROUGH THE ACTUAL CALIBRATION POINTS OF THIS TRANSDUCER.

OUR CALIBRATION STANDARDS ARE TRACEABLE TO THE N.I.S.T., (NBS).

CUSTOMER: UNIVERSITY OF MAINE
ORONO, ME 04469

THIS CALIBRATION SHEET SHOWS THE CHARACTERISTICS OF THE TRANSDUCER

DATE : 08-12-2002

MODEL : ALD-BOLT-1/2-2

SERIAL NO. : 220807

CAPACITY = 9220 LBS

EXCITATION = 10 VOLTS DC

RESISTANCE BETWEEN RED & BLACK WIRES =497 OHMS NOMINAL

RESISTANCE BETWEEN WHITE & GREEN WIRES= 350 OHMS NOMINAL

SAFE OVERLOAD = 150% OF RATED CAPACITY

ULTIMATE OVERLOAD = 250% OF RATED CAPACITY

NOMINAL TEMPERATURE EFFECT ON RATED OUTPUT (15-115 deg.F) *
= 0.08% / deg.F OF RATED OUTPUT

NOMINAL TEMPERATURE EFFECT ON ZERO BALANCE (15-115 deg.F) *
= 0.08% / deg.F OF RATED OUTPUT

* THIS DOES NOT APPLY TO GAGED BOLTS
OR TRANSDUCERS MADE OF MATERIALS OTHER THAN
17-4PH STAINLESS STEEL.

STRAIN GAGE TEMPERATURE LIMITS FOR HIGH/LOW TEMP. OPTION.
HIGH TEMP. = +450 degrees F. LOW TEMP. = -452 degrees F.
THESE TEMPERATURE EFFECTS ARE FOR FOIL STRAIN GAGES ONLY.
SEMICONDUCTOR STRAIN GAGES HAVE HIGHER TEMPERATURE SENSITIVITY

NUMBER OF CALIBRATION POINTS IS : 10
AT NO LOAD, INDICATOR OUTPUT READS 0 mV

	RUN #1			RUN #2	
POINT	LOAD	TRANSDUCER OUTPUT	POINT	LOAD	TRANSDUCER OUTPUT
#1	1844 LBS	4.34 mV	#6	1844 LBS	4.32 mV
#2	5532 LBS	12.94 mV	#7	5532 LBS	12.89 mV
#3	9220 LBS	21.61 mV	#8	9220 LBS	21.6 mV
#4	5532 LBS	12.97 mV	#9	5532 LBS	12.95 mV
#5	1844 LBS	4.32 mV	#10	1844 LBS	4.31 mV

CHARACTERISTICS PARTICULAR
TO THIS TRANSDUCER ARE :

NON LINEARITY = +/- .2 % F.S.

HYSTERESIS +/- .17 % F.S.

REPEATABILITY = +/- .14 % F.S.

RATED OUTPUT = 21.6 mV

SENSITIVITY = 2.16 mV/V

LOADCELL'S UNADJUSTED ZERO OFFSET = .13 mV

ADJUSTED INDICATOR ZERO OFFSET = 0 mV

CALCULATED VALUES USING THE BEST FIT
STRAIGHT LINE THROUGH THE EXPERIMENTAL POINTS

POINT	LOAD	TRANSDUCER OUTPUT
#1	922 LBS	2.2 mV
#2	1844 LBS	4.3 mV
#3	2766 LBS	6.5 mV
#4	3688 LBS	8.6 mV
#5	4610 LBS	10.8 mV
#6	5532 LBS	13 mV
#7	6454 LBS	15.1 mV
#8	7376 LBS	17.3 mV
#9	8298 LBS	19.4 mV
#10	9220 LBS	21.6 mV

SHUNT CALIBRATION DATA

LOAD CELL SERIAL NO. = 220807

SHUNT RESISTOR VALUE = 200000 OHMS

EXCITATION = 10 Vdc

SHUNT OUTPUT = 3.08 mV

SHUNT CONNECTION = RED and WHITE

EXCITATION = (+)RED and (-)BLACK

SIGNAL OUTPUT = (+)WHITE and (-)GREEN

WHEN USING AN ALD-MINI-UTC TENSION/COMPRESSION LOAD CELL THE SMOOTH FLAT SURFACE SHOULD NOT TOUCH ANYTHING. THE OTHER SIDE WITH THE CIRCLE NEAR THE OUTER EDGE IS THE BASE. IT IS OK TO MOUNT OTHER PARTS TO IT AND TO TOUCH THIS SURFACE ONLY.

WHEN CONNECTORS ARE SUPPLIED,
CONNECTOR PIN ASSIGNMENTS ARE:

A = BLACK (-) EXCITATION
B = WHITE (+) SIGNAL
C = RED (+) EXCITATION
D = GREEN (-) SIGNAL

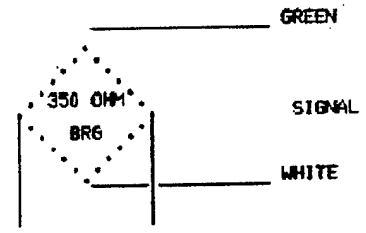

INTERNAL WHEATSTONE BRIDGE

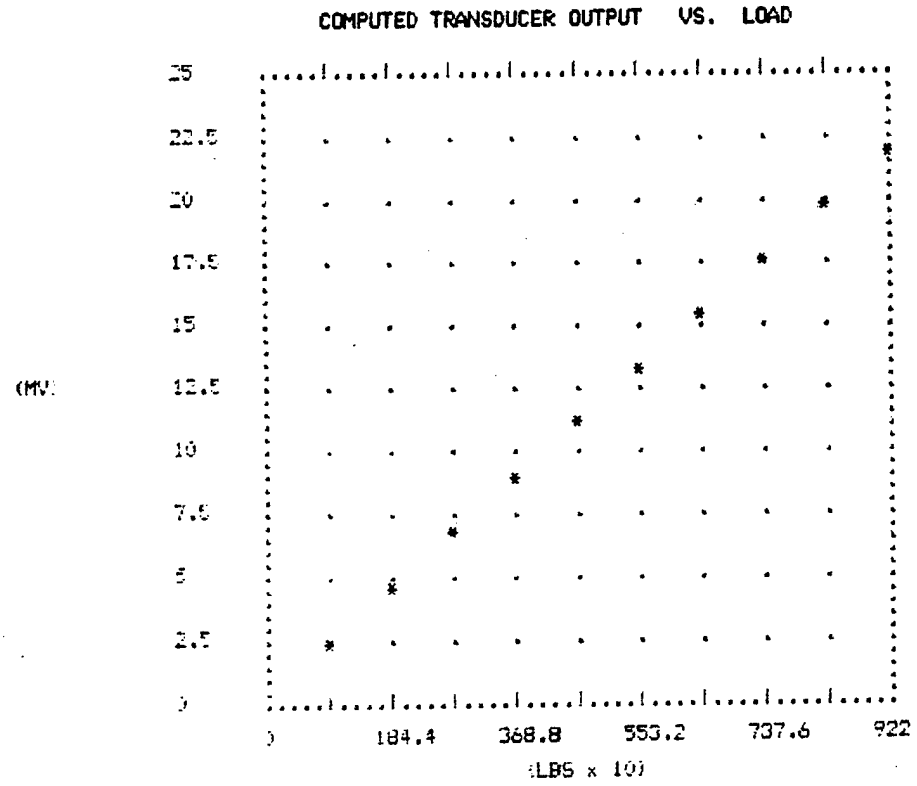
COMPUTED TRANSDUCER OUTPUT VS. LOAD
25
22.5
20
17.5
15
12.5
10
7.5
5
2.5
0
(MV)
0
184.4
368.8
553.2
737.6
922
(LBS x 10)

APPENDIX B

Siglab Information

The SigLab acquisition and processing hardware was designed by a team of engineers with over 60 years of combined experience in the measurement art. The 20-42 and 50-21 systems are highly optimized for the task of making fast, accurate measurements of electrical, mechanical, or acoustical signals and systems. The SigLab systems are complex and powerful with capabilities that should not be confused with PC add-in boards or audio entertainment devices such as the "Sound Blaster". The goals of measurement quality, speed, size, durability and expandability are well met with the SigLab measurement hardware platform.

The differential inputs have ten full-scale ranges (20mV to 10V) allowing accurate measurement of signals from far less than a millivolt to 20 volts peak to peak. These inputs are protected up to 30 volts rms and the overload detectors guarantee that your measurements are valid by trapping overload conditions that may not be apparent due to subsequent filtering operations. You can specify ac/dc coupling as well as the dc offset. Optional integrated ICP power transducer bias sources provide a constant 4mA current with a 22 volt compliance to directly power accelerometers, microphones, and force transducers. Additionally, your own signal conditioning circuitry can be inserted in SigLab beneath the top cover access panel.

A fourth-order analog low-pass filter precedes the sigma-delta A/D converter providing complete alias protection with only 0.03 dB of ripple. The sigma-delta conversion technology provide ultra linear, and low noise performance. The SigLab 50-21 boasts unmatched measurement quality with a guaranteed 95 dB spurious free dynamic range over its entire 50 kHz bandwidth.

A dedicated fixed point DSP filters and decimates the A/D data stream providing a selection of 13 alias-protected sampling rates down to 5 Hz. Either low-pass or band-pass filtering for narrow-band “zoom” analysis may be selected. Triggering circuitry

provides slope control and 17 selectable threshold levels. The trigger source can be an input channel, an output channel, or a rear panel digital input.

The trigger may also select unfiltered data thereby providing a reliable trigger even with short duration "impulses" often encountered in modal impact testing.

The output subsystem looks much like the input subsystem in reverse. The TMS320C31 floating point DSP feeds previously acquired data or data generated mathematically (e.g. by using MATLAB) to the function generator FIFO buffer. The fixed point DSP then interpolates and optionally translates this data before sending it to the highly linear D/A converter. The output subsystem's signal quality is comparable to the input subsystem. The DSP is also used to generate predefined functions: sine, square, sawtooth, triangle, impulse, random, and chirp. Level control and DC offset can be applied to the analog signal before going to the output buffer amplifier. The buffer can source and sink at least 20 mA, has a 50 ohm output resistance, and is unconditionally stable.

The TMS320C31 floating-point DSP chip performs real-time processing tasks such as FFTs, auto and cross-spectral averaging, and computation of transfer and other functions. A real-time operating system kernel is also executing in the C31 to orchestrate the flow of data within SigLab and between SigLab and the host PC via the SCSI interface. The system can be equipped with a generous amount of DRAM allowing gap free records of up to 15 million samples to be stored at the maximum sampling rate. Non-volatile memory (not shown) stores the input/output calibration factors. Except for a small boot program, all C31 code is downloaded from the host PC.

For expansion beyond four channels, SigLab's architecture allows interconnecting multiple units. The SigLab modules are linked by an external cable providing synchronous multi-channel capability. This Multi Unit Sync. subsystem manages the synchronization of all sampling clocks and trigger signals for the input and output channels. For normal operation SigLab is powered by a DC input between 12 and 15 volts. It can also run on its own internal NiCAD battery for a limited time.

APPENDIX C

ACX Actuator

CYMER | ACX Active Control eXperts
A Division of Cymer

Contact Us

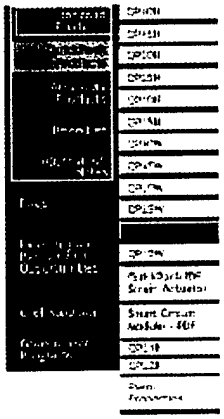

QuickPack® Actuator

Cat. No. QP10W

Model QP10W Specifications

Application type: strain actuator only
Device size (in): 2.00 x 1.50 x 0.015
Device weight (oz): 0.16
Active elements: 1 piezo wafer
Piezo wafer size (in): 1.81 x 1.31 x 0.010
Device capacitance: (µF): 0.10
Full scale voltage range (V): ±200

Functional Diagram

Device poled with positive voltage applied to pin 1. Pins 2 and 3 not connected.

Bonded Configuration

Full scale strain, extension (µε): ±276

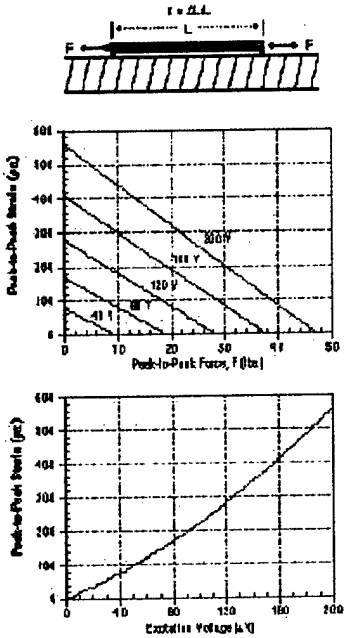

Price List

APPENDIX D

Dynamic Sensor Specifications

PCB PIEZOTRONICS™

Model 352B10

Product Type: Accelerometer

Miniature (0.7 gm), ceramic shear ICP® accel., 10 mV/g, 2 to 10k Hz, 10 ft integral cable

View large photo .

PERFORMANCE	ENGLISH	SI	
Sensitivity (±10 %)	10 mV/g	1.02 mV/(m/s²)	
Measurement Range	±500 g pk	±4905 m/s² pk	
Frequency Range (±5 %)	2 to 10000 Hz	2 to 10000 Hz	
Frequency Range (±10 %)	1 to 17000 Hz	1 to 17000 Hz	
Resonant Frequency	≥65 kHz	≥65 kHz	
Broadband Resolution (1 to 10000 Hz)	0.003 g rms	0.03 m/s² rms	[1]
Non-Linearity	≤1 %	≤1 %	[2]
Transverse Sensitivity	≤5 %	≤5 %	
ENVIRONMENTAL			
Overload Limit (Shock)	±10000 g pk	±98100 m/s² pk	
Temperature Range (Operating)	-65 to +250 °F	-54 to +121 °C	
Temperature Response	See Graph	See Graph	
ELECTRICAL			
Excitation Voltage	18 to 30 VDC	18 to 30 VDC	
Constant Current Excitation	2 to 20 mA	2 to 20 mA	
Output Impedance	≤200 ohms	≤200 ohms	
Output Bias Voltage	7 to 11 VDC	7 to 11 VDC	
Discharge Time Constant	0.3 to 1.0 sec	0.3 to 1.0 sec	
Settling Time (within 10% of bias)	<3 sec	<3 sec	
Spectral Noise (1 Hz)	1000 µg/√Hz	9810 (µm/s²)/√Hz	[1]
Spectral Noise (10 Hz)	300 µg/√Hz	2943 (µm/s²)/√Hz	[1]
Spectral Noise (100 Hz)	80 µg/√Hz	785 (µm/s²)/√Hz	[1]
Spectral Noise (1 kHz)	25 µg/√Hz	308 (µm/s²)/√Hz	[1]
PHYSICAL			
Sensing Element	Ceramic	Ceramic	
Sensing Geometry	Shear	Shear	
Housing Material	Titanium	Titanium	
Sealing	Hermetic	Hermetic	
Size (Height x Diameter)	0.32 in x 0.24 in	8.1 mm x 6.1 mm	
Weight	0.03 oz	0.7 gm	[1]
Electrical Connector	10-32 Coaxial Plug	10-32 Coaxial Plug	
Electrical Connection Position	Top	Top	
Cable Length	10 ft	3 m	
Cable Type	030 Coaxial	030 Coaxial	
Mounting	Adhesive	Adhesive	
SUPPLIED ACCESSORIES:			
Model 080A109 Petro Wax (1)			
Model 080A90 Quick Bonding Gel (1)			
Model ACS-1 NIST traceable frequency response (10 Hz to upper 5% point). (1)			
OPTIONAL VERSIONS			
W - Water Resistant Cable			
Temperature Range (Operating)	-20 to 220 °F	-29 to 104 °C	
Electrical Connector	Sealed Integral Cable	Sealed Integral Cable	
Cable Type	018 Coaxial	018 Coaxial	

All specifications are at room temperature unless otherwise specified.

NOTES:

[1] Typical.

[2] Zero-based, least-squares, straight line method.

Ceramic Shear ICP® Accelerometers

MINIATURE *(complete specifications are featured on page 14 to 15)*

Miniature accelerometers are especially well suited for applications demanding high frequency range, small size, and light weight.

- NHV studies
- printed circuit boards
- card cages and chassis
- brackets
- thin panels
- shrouds
- conduits
- bearings

Available Sensor Options:

Prefix	Description
A	Adhesive Mount
HT	High Temperature
J	Ground Isolated
M	Metric Mounting
W	Attached Water Resistant Cable
●	Popular Product (see page 1)

Designate option as prefix to model number, e.g., J352C66 specifies a unit with electrical ground isolated base.

Accessory key located on page 11

10

● **Model 352A10** (accessory key: ●)

- 10 mV/g sensitivity
- 1 Hz to 20 kHz frequency range
- 0.7 gram in weight
- Integral cable
- Adhesive mount

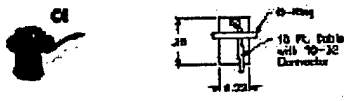

Model 352A10

Model 352A21 (accessory key: ❷③)

- 10 mV/g sensitivity
- 0.7 Hz to 13 kHz frequency range
- 0.6 gram in weight
- Adhesive mount
- Durable titanium housing
- Mating cable provided

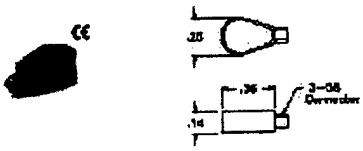

Model 352A21

● **Model 352C22** (accessory key: ❷③)

- 10 mV/g sensitivity
- 0.7 Hz to 13 kHz frequency range
- 0.5 gram in weight
- Adhesive mount
- Anodized aluminum housing
- Electrically ground isolated
- Mating cable provided

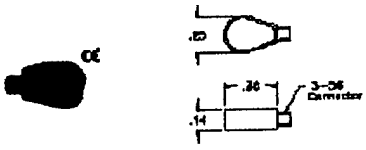

Models 352C22, 352A24

Model 352A24 (accessory key: ❷③)

- 100 mV/g sensitivity
- 0.8 Hz to 10 kHz frequency range
- 0.8 gram in weight
- Anodized, ground isolated, aluminum housing
- Mating cable provided

Model 740B02 Dynamic ICP® Piezoelectric Strain Sensor Specifications

Dynamic Performance	
Sensitivity[1]	50 mV/με
Amplitude Range[1]	±100 με pk
Environmental	
Operating Temperature	-65 to +250 °F (-54 to +121 °C)
Electrical	
Low Frequency Response	0.5 Hz
Excitation Voltage	20 to 30 VDC
Constant Current Excitation	2 to 20 mA
Output Bias	9 to 13 VDC
Mechanical	
Weight	0.02 oz (0.5 grams)
Size (W x L x H)	0.2 x 0.6 x 0.07 in. (5.1 x 15.2 x 1.8 mm)
Mounting	Adhesive
Cable	Integral Coaxial, 10 ft (3 m) Terminates in 10-32 threaded plug
Housing	Titanium
Sensing Element	Quartz

[1] Actual value depends upon thickness and stiffness of sensor structure interface.

This product is CE-marking compliant to European Union EMC Directive, based upon conformance testing to the following European norms:

- EN 50081-1: 1992 Emissions
- EN 50082-1: 1992 Immunity

SVS is the Shock and Vibration Sensors division of PCB Piezotronics, Inc., specializing in quartz, ceramic, charge, ICP®, and capacitive accelerometers. The divisional focus of SVS, combined with the strength and resources of PCB, offers customers exceptional customer service, 24-hour technical support, and an unconditional guarantee.

To obtain more information on this and other shock and vibration products contact SVS at 1-888-684-0013. For information on other PCB products, call 1-716-684-0001, or visit our web site at: www.pcb.com.

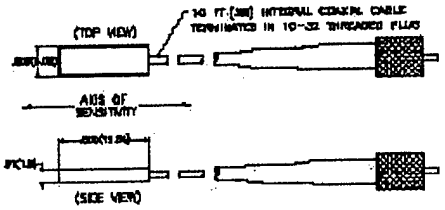

TYPICAL APPLICATION: An epoxy-bonded Model 740A02 Strain Sensor provides a control signal for an actively damped flexible robot manipulator, illustrated below. The electronic controller, with vibration feedback from the strain sensor, provides a signal to the amplifier, such that vibration amplitude is minimized. The active control system permits rapid settling time for a step rotation of the manipulator arm.

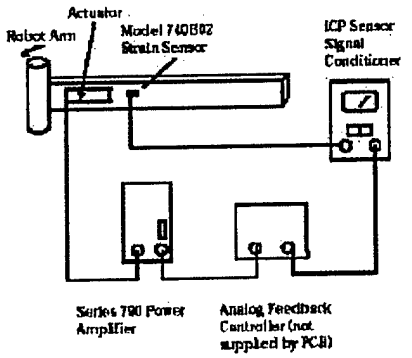

PCB PIEZOTRONICS SVS DIVISION

3425 Walden Avenue, Depew, NY 14043 • Telephone (716) 684-0001 • FAX (716) 685-3886 • e-mail: svssales@pcb.com

APPENDIX E

482A20 PCB ICP Sensor Signal Conditioner

Model Number	8 CHANNEL ICP® POWER SUPPLY	Revision: B
482A20		ECN #: 10813

ELECTRICAL						
Channels			8			
Transducer Excitation		volts	+24 ±1			
Excitation Current		mA	2-20 Adjustable			[1]
Voltage Gain (selectable)			x1, x10, x100			[3]
Gain Accuracy (all gains)		%	±1			
Frequency Response (-5%)		Hz	0.225 to 100 k			
Maximum Output Signal		volts	±10			
Output Impedance		ohms	<50			
Overload Detection		volts	±10			
Noise (spectral):	Typical	gain	x1	x10	x100	
	1 Hz	µV/√Hz	0.95	4.5	105	
	10 Hz	µV/√Hz	0.15	1.0	7.0	
	100 Hz	µV/√Hz	0.1	0.36	3.0	
	1 kHz	µV/√Hz	0.12	0.34	2.5	
	10 kHz	µV/√Hz	0.1	0.31	2.4	
Broadband Noise:	1 Hz-10 kHz (maximum)	µV	9.1	50	480	
Channel Isolation:	minimum	dB	72			
DC Offset (all gains)		mV	±50			
Power Required (50 to 400 Hz)		VAC/mA	90-130/500			
Alternate Power		VAC/mA	210-250/250			[2]
PHYSICAL						
Connectors:	Input	type	BNC Jack			
	Output	type	BNC Jack			
Size (L x W x H):		in	9.7 x 4.0 x 6.3			
		[cm]	[24,6 x 10,2 x 16,0]			
Weight		lb [gm]	6.1 [2 767]			

NOTES:
[1] Units supplied with current set at 4 mA ±0.6 mA.
[2] Unit is factory configured using internal jumpers when ordered with prefix "F". Example: F482A20.
[3] Units with serial number 139 or greater will power up to the same settings it had at power down.

SUPPLIED ACCESSORIES:
Model 017 AC Line Cord

In the interest of constant product improvement, we reserve the right to change specifications without notice.

ICP® is a registered trademark of PCB Piezotronics, Inc.

PCB PIEZOTRONICS GEP DIVISION

Drawn			Spec No. 482-1200-80
Engineer			
Sales			
Approved			Sheet 1 of 1

APPENDIX F

Damping Program

```
function damping_driver

%  This function finds the damping coefficients for a series of text files
%  A plot is generated of the damping coefficients vs. applied torque
%  functions fileread is used to open the respect text files,
%  and function Find_Damping actually computes the damping coefficients

%  DD is a matrix of applied torques
%  DD(1,1) = 0 is the finger tight file

%  Functions Called:
%  -Find_Damping


DD(1,1) = [0]';
DD(2:20,1) = [50 60 70 80 90 100 120 130 140 150 160 170 200 230 300 360 480 600
720]';

%  loop to compute damping coefficients

for i = 1:max(size(DD))


str1 = 't_';
str2 = num2str(DD(i));
str3 = '_inst_narrow.txt';

fstring = strcat(str1,str2,str3);
damping( i) = Find_Damping( fstring);
torque(i) = DD(i);
end

%  Plot the results
plot(torque,damping)
axis([0 800 0 .014])
Title('Fundamental Mode Damping Sensitivity to Torque')
ylabel('Damping Coefficient')
xlabel('Bolt torque in (in-lbs)')
grid on;
```

```
axis([0 720 0 .014])

function damping = Find_Damping(filename)

%  Function to compute the damping coefficient for the input TRANSFER
%  FUNCION text file.  Utilizes the 3-dB down method to estimate the
%  damping coefficient.  This function works only for finding the damping
%  coefficient for the maximum peak.  The best results are obtained with
%  the transfer function bracketed around the peak response corresponding
%  to modal damping coefficient of interest.

%  m-files called:
%  -fileread


%  load the file
q = fileread(filename);
freq = q(:,1);
mag = q(:,2);

%  Find the maximum magnitude value, and it's location.
[max_mag,I] = max(mag);
omega_d = freq(I);

%  Calculate the 2 dB down points
dB3 = 20*log10(1/sqrt(2));
TwodBmag = max_mag+dB3;

%  Find omega_a
%  ------------------------------------------------------------
n = I-1;
mag(n);
while mag(n) > TwodBmag;
   n = n-1;
end

if mag(n) == TwodBmag
   omega_a = freq(n);
else
   magLOW = mag(n);
   omegaLOW = freq(n);

   magHIGH = mag(n+1);
   omegaHIGH = freq(n+1);
```

```
   omega_a = (omegaLOW - omegaHIGH)*((TwodBmag - magHIGH)/(magLOW -
magHIGH)) + omegaHIGH;
end
%  ------------------------------------------------------------

%  Find omega_b
%  *****************************************************************
m = I+1;
mag(m);
while mag(m) > TwodBmag;
   m = m+1;
end

if mag(m) == TwodBmag
   omega_a = freq(m);
else
   magHIGH = mag(m);
   omegaHIGH = freq(m);

   magLOW = mag(m-1);
   omegaLOW = freq(m-1);

   omega_b = (omegaLOW - omegaHIGH)*((TwodBmag - magHIGH)/(magLOW -
magHIGH)) + omegaHIGH;
end
%  *****************************************************************

%  Compute the damping ratio
damping = (omega_b - omega_a)/(2*omega_d);


disp(TwodBmag)
disp(omega_a)
disp(omega_b)
disp(omega_d)
```

```
function res=fileread(filename)

%  This function is used to read the TRANSFER FUNCTION output generated by
%  Siglab.  The Siglab text file is opened, and the text preceding the
%  data is ignored.

format long g
[fid , message] = fopen(filename, 'rt');
dummy = fscanf(fid,'%c%[^\n]');
dummy = fscanf(fid,'%c%[^\n]');
dummy = fscanf(fid,'%s',[1,6]);
res=fscanf(fid,'%g');
res=transpose(reshape(res,3,[]));
status = fclose(fid);
```

REPORT DOCUMENTATION PAGE

Form Approved
OMB No. 0704-0188

1. REPORT DATE *(DD-MM-YYYY)*	2. REPORT TYPE	3. DATES COVERED *(From - To)*
14-April-2003	Project Report	22-June-2001 to 14-April-2003

4. TITLE AND SUBTITLE

Detection of Bolt Stress Relaxation in Hybrid Bolted Connections

5a. CONTRACT NUMBER

5b. GRANT NUMBER
N00014-01-1-0916

5c. PROGRAM ELEMENT NUMBER

6. AUTHOR(S)

Mewer, Richard
Vel, Senthil S. and
Caccese, Vincent

5d. PROJECT NUMBER

5e. TASK NUMBER

5f. WORK UNIT NUMBER

7. PERFORMING ORGANIZATION NAME(S) AND ADDRESS(ES)

University of Maine
Office of Research and Sponsored Programs
5717 Corbett Hall
Orono, ME 04469-5717

8. PERFORMING ORGANIZATION REPORT NUMBER

UM-MACH-RPT-01-07

9. SPONSORING/MONITORING AGENCY NAME(S) AND ADDRESS(ES)

Office of Naval Research
Ballston Center Tower One
800 North Quincy St.
Arlington, VA 22217-5660

10. SPONSOR/MONITOR'S ACRONYM(S)
ONR

11. SPONSORING/MONITORING AGENCY REPORT NUMBER

12. DISTRIBUTION AVAILABILITY STATEMENT

Approved for Public Release, Distribution is Unlimited

13. SUPPLEMENTARY NOTES

14. ABSTRACT

The effort summarized in this report focuses upon real time detection of stress relaxation in bolted connections in hybrid structures. A proof-of-concept test bed for this effort consists of a 24-½ inch square plate made of Eglass/vinyl ester composite. Several interrogation techniques were employed and compared including: 1) low frequency modal analysis; 2) high frequency transfer functions and 3) high frequency transmittance functions. Each of these techniques employed a piezoelectric actuator bonded to the panel so to deliver a characterized disturbance in a controlled manner. The technique using transmittance functions to evaluate changes in bolt tensioning level shows the most promise.

15. SUBJECT TERMS

Composites; Hybrid Structures; Composite Construction; Connections; Structural Monitoring; Vibration Analysis; Damage Detection

16. SECURITY CLASSIFICATION OF:			17. LIMITATION OF ABSTRACT	18. NUMBER OF PAGES	19a. NAME OF RESPONSIBLE PERSON
a. REPORT	b. ABSTRACT	c. THIS PAGE			Vincent Caccese
U	U	U	UU	74	19b. TELEPONE NUMBER *(Include area code)* (207) 581-2131